COMPOSITE MATERIALS LABORATORY

PURDUE UNIVERSITY
School of Aeronautics and Astronautics
West Lafayette, Indiana 47907

CML 88-3

CHARACTERIZATION OF ELASTIC-PLASTIC PROPERTIES OF AS4/APC-2 THERMOPLASTIC COMPOSITE

C. T. Sun and K. J. Yoon

August 1988

A technical report prepared for
NASA Langley Research Center,
Hampton, Virginia

This research was supported by
NASA Research Grant NAG-1-825.

Abstract

Elastic and inelastic properties of AS4/APC-2 composites were characterized with respect to temperature variation by using a one parameter orthotropic plasticity model and a one parameter failure criterion. Simple uniaxial off-axis tension tests were performed on coupon specimens of unidirectional AS4/APC-2 thermoplastic composite at various temperatures. To avoid the complication caused by the extension-shear coupling effect in off-axis testing, new tabs were designed and used on the test specimens. The experimental results showed that the nonlinear behavior of constitutive relations and the failure strengths can be characterized quite well using the one parameter plasticity model and the failure criterion, respectively.

1. Introduction

AS4/APC-2 is a high-performance thermoplastic composite material based on polyether-ether-keton (PEEK) reinforced with AS4 graphite fiber. Compared with epoxy-based composite materials, AS4/APC-2 has improved impact toughness and damage tolerance as well as good creep and fatigue resistance. It also has good environmental properties, such as high temperature performance (Tg : 290°F), low water absorption and excellent solvent and fire resistance. This material offer to the industry great flexibility in fabrication processing, storage and repair.

The increase in toughness and resistance of AS4/APC-2 is from the increased ductility of APC-2 PEEK resin. The greater ductility of the matrix implies more pronounced plasticity or visco-elastic-plasticity in the matrix-dominant deformation. Therefore, characterizing the nonlinear rate-dependent stress-strain relations may be needed in the design and application of thermoplastic composite structures.

Many fiber composites exhibit physically nonlinear behavior. A number of models have been used to describe the nonlinear stress-strain relationship. Hahn and Tsai [1] employed a complementary elastic energy density function which contained a biquadratic term for in-plane shear stress. As a result, the stress-strain relation is linear in simple longitudinal and transverse extensions. Moreover, the shear strain is a quadratic polynomial function in the shear stress, which is unsuitable for describing the nonlinear behavior exhibited by many composites.

The physical nonlinearity in fiber composites can also be considered a plastic behavior. Dvorak and Bahei-El-Din [2-3] used a micromechanical model consisting of elastic filaments of vanishing diameters and an elastic-plastic matrix. An elastic-plastic continuum model was developed for which the constitutive relations depend on the constituent properties, their volume fractions, and mutual constraints between the phases associated with the geometry of the microstructure.

Inherent in these micromechanical models is the need to know the constituent material properties, fiber array, and fiber matrix interfacial condition. As noted in [4], the in situ matrix property could be quite different from that of the bulk matrix material. Consequently, adjustment of the matrix property in the micromechanical model is often necessary to yield good results. Another difficulty encountered in formulating micromechanical models lies in the 3-D elastic constants of the fiber which are extremely difficult to measure because of their small size. Recently, Johnson et al [5] indicated that the fiber-matrix interfacial bond in some metal-matrix composites is very weak as opposed to the perfect bond assumed in developing these micromechanical models.

For unidirectional composites, their plastic behavior is orthotropic. Sun et al proposed a three parameter plasticity model[6] and a one parameter plasticity model[7], parameters of which can be obtained from the simple uniaxial tension tests of off-axis specimens. They concluded that one parameter plasticity model is most suitable for describing the nonlinear behavior of composites exhibiting little plasticity in the fiber direction. This model is very attractive for characterizing the inelastic properties of continuous fiber reinforced composites at elevated temperature environments for its simple testing method to get the parameter.

The present study characterizes the elastic- plastic properties of the AS4/APC-2 composites with respect to temperature variation using the one parameter plasticity model and failure criterion.

2. Experimental Procedures

Specimens and Tabs

The 0°, 15°, 30°, 45°, and 90° coupon specimens were cut from the $[0_{10}]$ panels; the thickness was 0.05 ± 0.001 inch. The specimen length was 10.0 inch and the width was 0.75 ± 0.01 inch.

Rigid glass/epoxy tabs were used in testing 0° and 90° coupon specimens where extension shear coupling is absent; newly designed shear deformable flexible tabs were used in testing 15°, 30° and 45° coupon specimens where extension shear coupling exists. The specimen geometry is shown in Fig. 1.

New Tab for Off–Axis Testing

Among the many test methods for characterizing the mechanical properties of fiber reinforced composite materials, the off-axis coupon test seems attractive because of its easy specimen fabrication, simple data reduction, and no special equipment requirement. In order to extract material constants from an off-axis test, it is assumed that a uniform state of stress exists throughout the test section. One problem with off-axis tests of unidirectional composites is the presence of extension-shear coupling resulting from the anisotropy of the material. Since shear deformation is constrained at the conventional rigid grip of the testing machine, bending is induced in the specimen as are nonuniform stresses [8,9].

To solve the problem, the load must be applied in a way which allows shear deformation to occur. With this in mind Sun and Berreth [10] developed a shear deformable flexible tab using silicon rubber reinforced with bi-directional E-glass knit. They demonstrated that the use of this tab could produce an almost uniform stress field in off-axis coupon specimens with conventional hydraulic grips.

In these experiments two kinds of flexible matrix systems were used together with fiberglas knit for the new shear deformable tabs. The silicon rubber matrix tab used in [10] was too weak to transmit enough load at elevated temperatures. The flexible epoxy system (Flex Epoxy 103, Thermoset Plastic Inc.) whose flexibility can be tailored by choosing the ratio of resin and hardener, was used as the matrix of the tab. This tab was used for tests at room temperature and 150°F. The FM1000 adhesive film (thickness : 0.01 inch, American Cyanamid Co.) was used to fabricate the second kind of tab used for

tests at 250°F and 350°F.

Tab Fabrication Procedure

Three fiberglas knit/flexible matrix panels (12 in x 12 in) were fabricated. A flexible epoxy matrix panel whose mixing ratio of resin and hardener was 1:2 was made for the room temperature test. Another flexible epoxy panel, mixing ratio 1:1.5, was made for the 150°F test.

A layer of release ply was laid on a tool plate, and one ply of unidirectional Kevlar 49/Epoxy was laid to reinforce the flexible tab in the transverse direction. Two plies of fiberglas knit were then cut and placed over the Kevlar 49/Epoxy ply. Six ounces of epoxy resin were mixed and spread evenly over the knit. A second layer of release ply and a caul plate were placed over the panel. The panel was then placed in a vacuum bag and cured in an autoclave. The panels were cured at 200°F and 25 inch Hg vacuum for an hour. The heating rate was 4°F/min. Another tab panel for the 250°F and 350°F tests was fabricated using four sheets of FM1000 adhesive film and two sheets of fiberglas knit. It was cured according to the FM1000 cure schedule provided by American Cynamid. The resulting panels had a nominal thickness of 0.08 inch.

Test Procedures

Uniaxial tension tests were performed using the closed-loop-servo hydraulic MTS 810 machine at 75°F, 150°F, 250°F, and 350°F. The schematic of the testing and data collection systems is shown in Fig. 2. The specimen was heated in the heating chamber (Model F–2–CH–CO_2 , Thermotron Corp.). The specimen was held in MTS 647 high temperature hydraulic wedge grips which can be used up to 350°F. The grip pressure was set at 1200 psi for the rigid tab specimen and at 600 psi for the flexible tab specimen to avoid crushing the specimen by the gripping force. A gripping test showed that the 15° coupon specimen was crushed at 800 psi grip pressure.

All tests were performed at a constant strain rate control of 300 με/min. Longitudinal and transverse strains were measured by strain gages (Micro Measurement EA-13-125AC-350) mounted at the center of specimen (Fig. 1). The measured analog signals were converted into digital signals. The signals were stored and analyzed by a micro-computer data system.

3. Experimental Results and Discussion

The stress-strain curves of 0°, 15°, 30°, 45°, 90° coupon specimens tested at 75°F, 150°F, 250°F, and 350°F are shown in Figs. 3-4. Figures 3 present the stress-strain curves for all off-axis specimens at each testing temperature, and Figs. 4 show the variation of stress-strain relations for different temperatures at each off-axis angle.

Modulus and Strength

The apparent tensile moduli and strengths of each off-axis coupon specimen are summarized in Table 1. The temperature effects on apparent moduli and strength are shown in Fig. 5 and Fig. 6, respectively.

It is noted that the longitudinal modulus does not change with respect to temperature variation, but the apparent moduli of other off-axis specimens drop to 80-85% of the modulus of room temperature at 250°F, and to 45-60% at 350°F. The decreasing rate of the apparent moduli of off-axis specimens becomes higher over 250°F. It is evident that the longitudinal modulus remained unchanged since it is dominanted by the graphite fiber which is not sensitive to temperature variation. Since the transverse property is dominanted by the APC-2 matrix, which is sensitive to temperature variation, the shear and the transverse moduli decrease significantly as temperature increases.

Generally, the modulus of polymer matrix decreases slowly until the temperature is elevated to the glass transition point, beyond which it drops very rapidly. The glass transition temperature of APC-2 thermoplastic is 290°F; and, thus, the sharp reduction of the transverse modulus over 250°F is expected.

Apparent strengths are shown in Table 1 and Figure 6. The longitudinal strength does not change with temperature variation as expected. The apparent strengths of off-axis specimens drop to 40-48% of the room temperature strength at 350°F. However, the rate of reduction in the apparent strengths of off-axis specimens does not seem sensitive to temperature near the glass transition temperature of the PEEK resin.

4. One Parameter Plasticity Model

In this study, a one-parameter plastic potential of the form

$$2f = \sigma_{22}^2 + 2a_{66}\sigma_{12}^2 \tag{1}$$

is used which was proposed by Sun et al[7]. From this plastic potential, the plastic strain increments are derived:

$$\begin{Bmatrix} d\varepsilon_{11}^p \\ d\varepsilon_{22}^p \\ d\gamma_{12}^p \end{Bmatrix} = \begin{Bmatrix} 0 \\ \sigma_{22} \\ 2a_{66}\sigma_{12} \end{Bmatrix} d\lambda \tag{2}$$

where γ_{12} is an engineering shear strain. The corresponding effective stress and effective plastic strain increments are defined by

$$\bar{\sigma} = \left[\frac{3}{2}(\sigma_{22}^2 + 2a_{66}\sigma_{12}^2) \right]^{\frac{1}{2}} \tag{3}$$

and

$$d\bar{\varepsilon}^p = \left[\frac{2}{3}(\sigma_{22}^2 + 2a_{66}\sigma_{12}^2) \right]^{\frac{1}{2}} d\lambda \tag{4}$$

respectively. The complete orthotropic plastic flow rule is defined if the parameters a_{66} and $d\lambda$ are determined.

Off–Axis Tension Test

To determine $d\lambda$, the effective stress-effective plastic strain relation must be established. This can be accomplished from the result of tension tests on off-axis specimens.

Let x-axis be the uniaxial loading direction which makes an angle θ with the fiber direction x_1-axis. The stresses referring to the material principal axes (x_1 and x_2) are related to the applied uniaxial stress σ_x as

$$\begin{aligned} \sigma_{11} &= \cos^2\theta\, \sigma_x \\ \sigma_{22} &= \sin^2\theta\, \sigma_x \\ \sigma_{12} &= -\sin\theta\cos\theta\, \sigma_x \end{aligned} \tag{5}$$

Substitution of equations (5) into (3) and (9) yields

$$\bar{\sigma} = h(\theta)\, \sigma_x \tag{6}$$

where

$$h(\theta) = \sqrt{\frac{3}{2}} \left[\sin^4\theta + 2a_{66}\sin^2\theta\cos^2\theta \right]^{\frac{1}{2}} \tag{7}$$

Using a similar coordinate transformation for strains and the definition for $d\bar{\varepsilon}^p$ as given by equation (4), we obtain

$$d\bar{\varepsilon}^p = d\varepsilon_x^p/h(\theta) \quad \text{or} \quad \bar{\varepsilon}^p = \varepsilon_x^p/h(\theta) \tag{8}$$

Thus, the desired relation between $\bar{\sigma}$ and $\bar{\varepsilon}^p$ can now be obtained from the experimentally obtained relation between σ_x and ε_x^p. It follows that

$$\frac{d\bar{\sigma}}{d\bar{\varepsilon}^p} = h^2(\theta)\frac{d\sigma_x}{d\varepsilon_x^p} \tag{9}$$

and

$$d\lambda = \frac{3}{2}\frac{1}{h^2(\theta)}\frac{d\varepsilon_x^p}{d\sigma_x}\frac{d\sigma_x}{\sigma_x} \tag{10}$$

Since the $\bar{\sigma}$–$\bar{\varepsilon}^p$ relation should be unique in monotonic loading for the given material, the parameter a_{66} must be chosen so that the resulting $\bar{\sigma}$–$\bar{\varepsilon}^p$ relation is independent of θ.

The procedure for determining the one-parameter plasticity model becomes very simple. In theory, only two off-axis specimens with different θ's are required to determine a_{66}. Note that for $\theta = 90^\circ$, $h(\theta) = \sqrt{3/2}$ and, thus, the stress-strain relation for the 90°-specimen is not affected by the choice of a_{66} and can be conveniently used to construct the master effective stress-effective plastic strain curve for the composite.

Experimental results indicate that for fiber composites there is no well defined yield point. In view of this, the master effective stress-effective plastic strain curve can be fitted as a power law,

$$\bar{\varepsilon}^p = A(\bar{\sigma})^n \qquad (\bar{\sigma} \text{ in ksi}) \tag{11}$$

which implies that yielding occurs from the start of loading.

Parameter and Coefficients Evaluation

The parameter a_{66}, coefficients A and n may be functions of temperature, strain rate and any other environmental factors. In this study, the effects of temperature on a_{66}, A and n of AS4/APC-2 composites are investigated.

The effective stress-plastic strain relations of all off-axis specimens at 75°F, 150°F, 250°F, and 350°F are shown in Figs. 7-a, b, c and d, respectively. They show that the effective stress-effective plastic strain data of each off-axis angle are collapsed into one curve with $a_{66} = 1.5$ for all temperatures. This indicates that the plastic orthotropy of

AS4/APC-2 is independent of temperature.

By taking the logarithm for the power law, equation (11), and using linear curve fitting, the coefficients A and n can be determined. The logarithms of effective stress and plastic strain and the fitted line are shown in Figs. 8-a, b, c, and d. The coefficients summarized in Table 2 show that n = 7.0 is adequate for temperatures up to 250°F, and coefficient A is related to temperature as

$$\ln(A) = 0.023T - 24.0 \tag{12}$$

for temperatures below the glass transition point (Figure 9).

The stress-strain curve in loading can be predicted using the following equation.

$$\varepsilon_x = \frac{\sigma_x}{E_x} + \varepsilon_x^p \tag{13}$$

$$= \frac{\sigma_x}{E_x} + \left[h(\theta)\right]^{n+1} A\sigma_x^n$$

Figures 10-a, b, c, and d show the total stress-strain curves, experimental and predicted, for the off-axis specimens at each testing temperature. Agreement between data and prediction is quite good.

Plastic Poisson's Ratio

The validity of a_{66} can be checked by the comparison of the plastic Poisson's ratios obtained from theory and experiment. The plastic Poisson's ratio is defined as

$$\nu_\theta^p = -\frac{d\varepsilon_y^p}{d\varepsilon_x^p} \tag{14}$$

From equations (2) and (5) and the transformation law on strain components, the plastic strain increments in x-direction and y-direction can be obtained, which in turn leads to

$$v_\theta^p = \frac{(2a_{66}-1)\cos^2\theta}{\sin^2\theta+2a_{66}\cos^2\theta} \tag{15}$$

In the off-axis tension test, longitudinal and transverse strains are measured, from which the plastic strains can be obtained and, thus, the plastic Poisson's ratio.

Table 3 and Figure 11 show that the predicted plastic Poisson's ratio with $a_{66} = 1.5$, and the experimental data match well up to 250°F except for the data from the 30° off-axis specimen tested at 250°F.

5. One Parameter Failure Criterion

We propose a dual mode failure criterion for the AS4/APC-2 composite. For fiber breakage, the failure criterion is assumed to be

$$\sigma_{11} \geq X \tag{16}$$

where X is the longitudinal strength. For matrix-dominated failure, the criterion is given by

$$\sigma_{22}^2 + 2a_{66}^*\sigma_{12}^2 = k_{cr}^2 . \tag{17}$$

where k_{cr} is a critical value and a_{66}^* a strength orthotropy parameter to be determined.

From equation (17), it is easy to derive the following relations:

$$k_{cr} = Y \quad , \quad 2a_{66}^* = \frac{Y^2}{S^2} \tag{18}$$

Thus, criterion (17) can be determined by measuring Y and S independently. Alternatively, the values of k_{cr} and a_{66}^* can be determined from the off-axis test results. In the latter case, the in-plane shear strength S can be obtained from equation (18).

Parameters a_{66}^* value k_{cr} were examined for temperature variation. It was found that the a_{66}^* is not sensitive to temperature variation (below T.G.), but k_{cr} decreases as temperature increases.

For the AS4/APC-2 composite, we recommend the use of

$$a_{66}^{*} = 0.74 \tag{19}$$

for temperatures below T.G.

Plotting k_{cr}^2 versus temperature as shown in Fig. 12, we found that k_{cr}^2 can be fitted as a linear function of temperature, i.e.,

$$k_{cr}^2 = -0.58T + 236 \tag{20}$$

Note that in the above equation k_{cr} is in ksi and T is in °F.

The experimental data and the predicted strengths from the one parameter criterion and Tsai-Hill criterion are compared in Figs. 13-a, b, c, and d. The two criteria agree except for small off-axis angles.

To further compare the Tsai-Hill failure criterion and the one parameter failure criterion in the small off-axis angle region, the 5° off-axis specimen was tested at room temperature. Table 5 shows that the apparent strength predicted by the one parameter failure criterion is more accurate than the Tsai-Hill failure criterion.

The in-plane shear strength can be obtained from the apparent strengths of off-axis specimens using either the Tsai-Hill failure criterion or the one parameter failure criterion. In the Tsai-Hill failure criterion, the shear strength is given by

$$S = \left[\frac{1}{\frac{1}{\sigma_x^2} - \left[\frac{\cos^2\theta}{X}\right]^2 - \left[\frac{\sin^2\theta}{Y}\right]^2 + \left[\frac{\sin^2\theta}{X}\right]\left[\frac{\cos^2\theta}{X}\right]} \right]^{\frac{1}{2}} \tag{21}$$

where σ_x is the apparent strength of the off-axis specimen with angle θ. In the one parameter failure criterion shear strength can be expressed as

$$S = \left[\frac{Y^2}{2a_{66}^*} \right]^{\frac{1}{2}} \tag{22}$$

Table 6 shows that the shear strengths calculated from equation (21) and equation (22) are almost the same.

6. Conclusion

Elastic-plastic behavior of AS4/APC-2 thermoplastic composite can be well characterized by using the one parameter plasticity model. It was found that the orthotropic plasticity parameter a_{66} and the power index n are not affected by temperature variation, and the logarithm of coefficient A varies linearly with temperature up to the glass transition temperature.

The failure strength of off-axis specimens can be predicted by using the one parameter failure criterion. Temperature effects on the strength of off-axis specimens can be described with the constant strength orthotropy parameter a_{66}^* and the critical potential value k_{cr}^2, which has a linear relationship with temperature variation. For specimens with small off-axis angles the one parameter failure criterion is more accurate than the Tsai-Hill failure criterion.

REFERENCES

1. Hahn, H.T. and Tsai, S.W., "Nonlinear Elastic Behavior of Unidirectional Composite Laminae," *Journal of Composite Materials,* Vol. 7, 1973, pp. 102-118.
2. Dvorak, G.J. and Bahei-El-Din, Y.A., "Elastic-Plastic Behavior of Fibrous Composites," *Journal of Mechanics and Physics of Solids,* Vol. 27, 1979, pp. 51-72.
3. Dvorak, G.J. and Bahei-El-Din, Y.A., "Plasticity Analysis of Fibrous Composites," Journal of Applied Mechanics, Vol. 49, 1982, pp. 327-335.
4. Bahei-El-Din, Y.A. and Dvorak, G.J., "Plastic Deformation of a Laminated Plate with a Hole," *Journal of Applied Mechanics,* Vol. 47, 1980, pp. 827-832.
5. Johnson, W.S., Lubowinski, S.J., Highsmith, A.L., Brewer, W.D. and Hoogstraten, C.A., "Mechanical Characterization of SCS6/Ti-15-3 Metal Matrix Composites at Room Temperature," NASP Technical Memorandum 1014, NASA-Langley Research Center, Hampton, Virginia, 1988.
6. Kenaga, D., Doyle, J.F. and Sun, C.T., "The Characterization of Boron/Aluminum Composite in the Nonlinear Range as an Orthotropic Elastic-Plastic Material," *Journal of Composite Materials,* Vol. 21, 1987, pp. 516-531.

7. Sun, C.T. and Chen, J.L., "A Simple Flow Rule for Characterizing Nonlinear Behavior of Fiber Composites," *Proceedings of the Sixth International Conference on Composite Materials,* Imperial College, London, England, July 20-25, 1987, pp. 1250-1259.

8. Rizzo, R.R., "More on the Influence of End Constraints on Off-Axis Tensile Tests," *J. Composite Materials,* Vol. 3, No. 4, 1969, p. 202.

9. Pagano, N.J., and Halpin, J.C., "Influence of End Constraints in the Testing of Anisotropic Bodies," *J. Composite Materials,* Vol. 2, No. 1, 1968, p. 18.

10. Barreth, S., Sun, C.T., "A New End Tab Design for Off-axis Tension Tests of Composite Materials," Thesis of M.S. Degree, Purdue University, 1986.

Table 1. Apparent elastic moduli and strengths

Angle (θ)	Temp.	Modulus(msi)	Strength(ksi)	Poisson's Ratio
0°	75°F	18.52	309.2	0.32
	150°F	18.80	311.5	0.33
	250°F	18.60	302.6	0.32
	350°F	18.50	293.4	0.34
15°	75°F	7.91	46.0	0.37
	150°F	7.27	38.3	0.34
	250°F	6.67	30.1	0.36
	350°F	4.80	21.2	0.38
30°	75°F	3.63	24.5	0.28
	150°F	3.30	20.8	0.27
	250°F	2.96	16.5	0.27
	350°F	1.64	11.2	0.41
45°	75°F	2.27	18.2	0.19
	150°F	2.13	15.5	0.17
	250°F	1.89	11.6	0.17
	350°F	1.05	7.1	0.25
90°	75°F	1.49	13.8	0.022
	150°F	1.39	12.3	0.023
	250°F	1.20	9.4	0.022
	350°F	0.71	5.8	0.021

Table 2. Coefficients A and n for temperature variation

Temp. / Coeff.	75°F	150°F	250°F	350°F
n	7.0	7.0	7.0	2.9
A	2.07×10^{-10}	1.53×10^{-9}	1.25×10^{-8}	2.05×10^{-3}
ln(A)	-22.33	-20.3	-18.2	-6.19

Table 3. Plastic Poisson's ratio

Temp. / Angle	75°F	150°F	250°F	350°F	from Theory
15°	0.673	0.646	0.698	1.074	0.650
30°	0.636	0.656	0.804	1.082	0.600
45°	0.562	0.544	0.517	0.848	0.500

Table 4. a_{66}^{*} and k_{cr}^{2} for temperature variation

Temp. / Parameter / Angle	75°F		150°F		250°F		350°F	
	a_{66}^{*}	k_{cr}^{2}	a_{66}^{*}	k_{cr}^{2}	a_{66}^{*}	k_{cr}^{2}	a_{66}^{*}	k_{cr}^{2}
15°	0.69		0.79		0.75		0.56	
30°	0.68		0.77		0.71		0.55	
45°	0.66		0.76		0.82		0.83	
Average	0.68	190	0.77	151	0.76	89	0.65	34

Table 5. Comparison of apparent strength of 5° off-axis specimen

Spec. No.	Experiment	Tsai-Hill	One Parameter
1	125.3		
2	135.4		
3	139.1		
Average	133.3	125.2	135.9

* unit : ksi

Table 6. Shear strength of each off-axis specimen for temperature variation

Temp. / Criteria / Angle	75°F		150°F		250°F		350°F	
	TH*	OP**	TH	OP	TH	OP	TH	OP
15°	11.9	11.8	9.9	9.8	7.7	7.7	5.5	5.5
30°	11.8	11.8	9.9	9.9	8.0	7.9	5.5	5.5
45°	12.1	12.0	10.0	10.0	7.4	7.4	4.5	4.5
Average	11.9	11.8	9.9	9.9	7.7	7.7	5.2	5.2

* From Tsai-Hill failure criterion

** From one parameter failure criterion

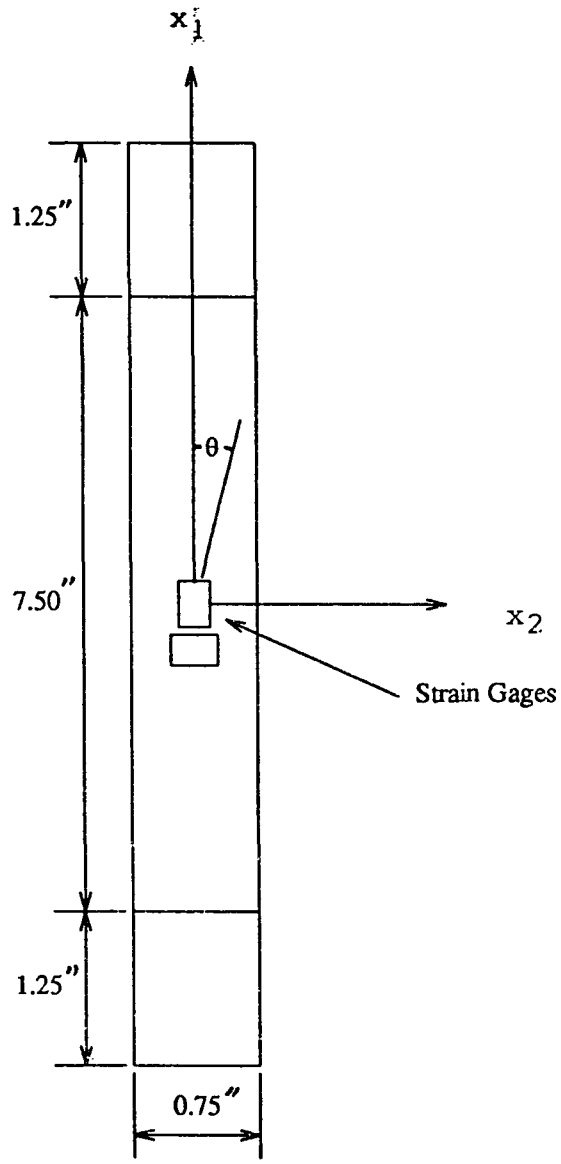

Fig.1. Specimen geometry and position of gages

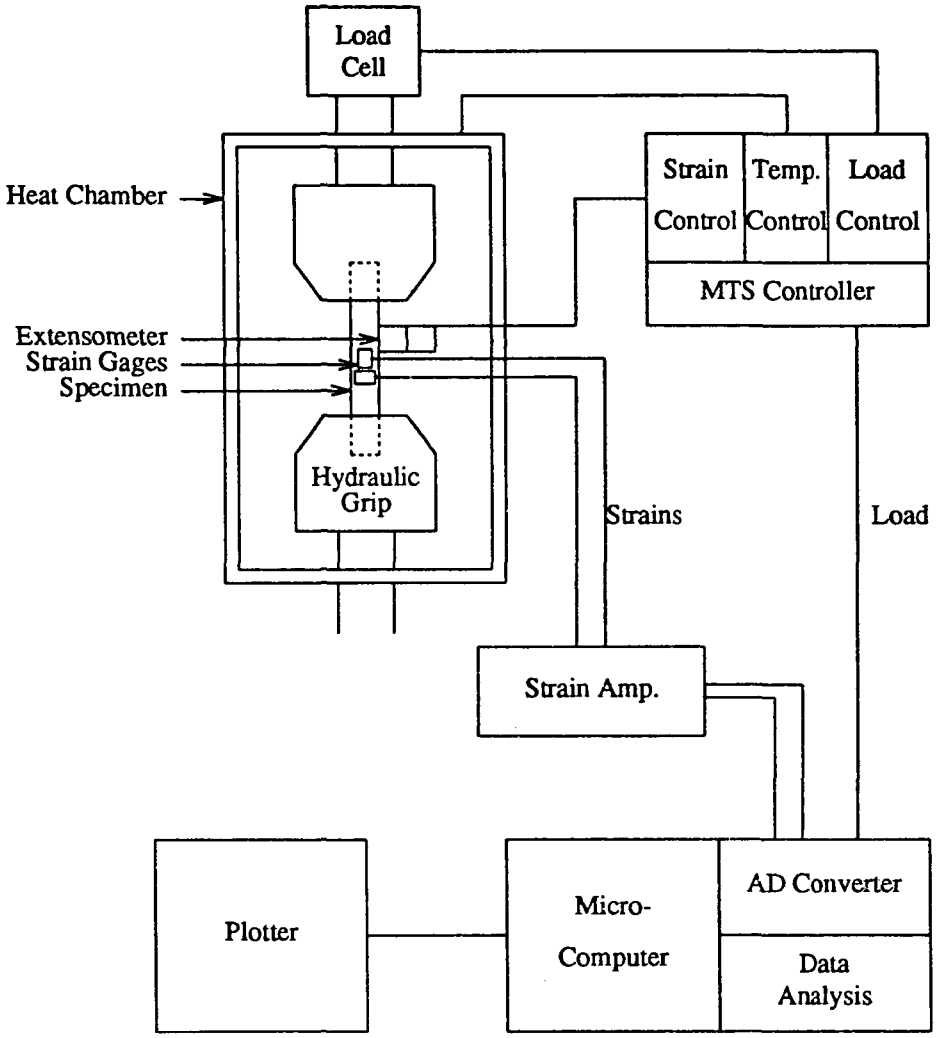

Fig.2. Schematic for testing system

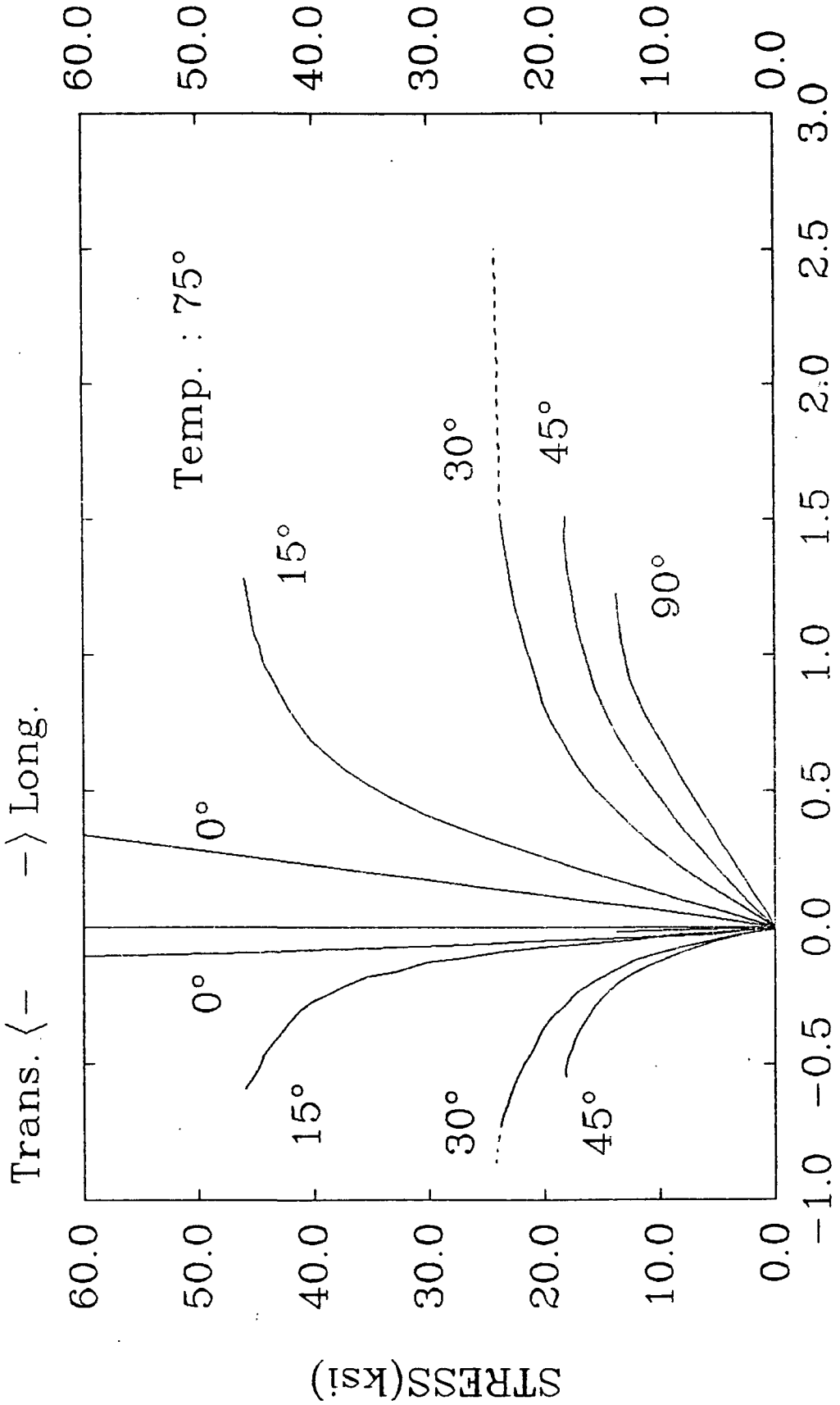

Fig. 3-a. Stress-strain curves for off-axis specimens at 75°F.

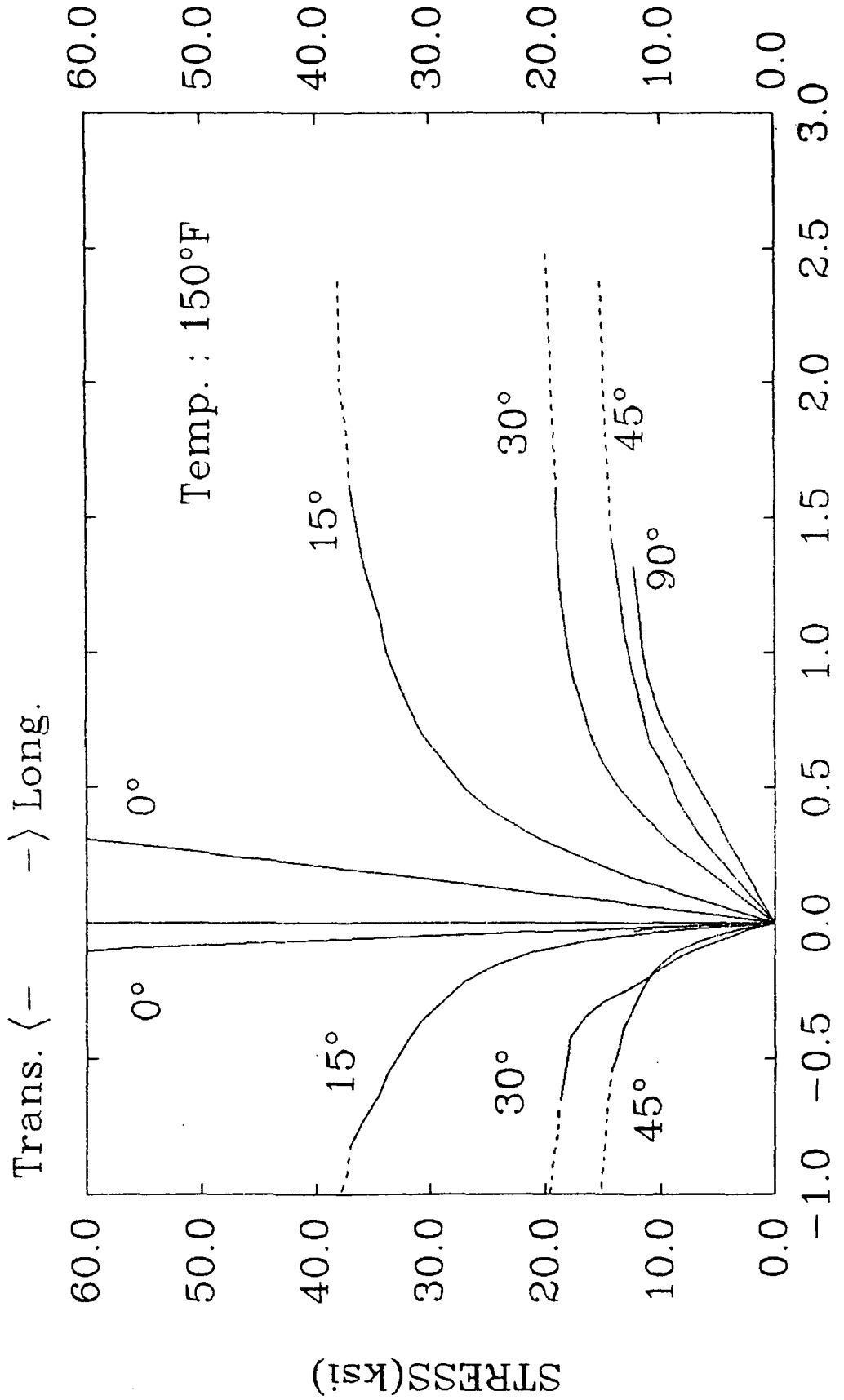

Fig. 3-b. Stress-strain curves for off-axis specimens at 150°F.

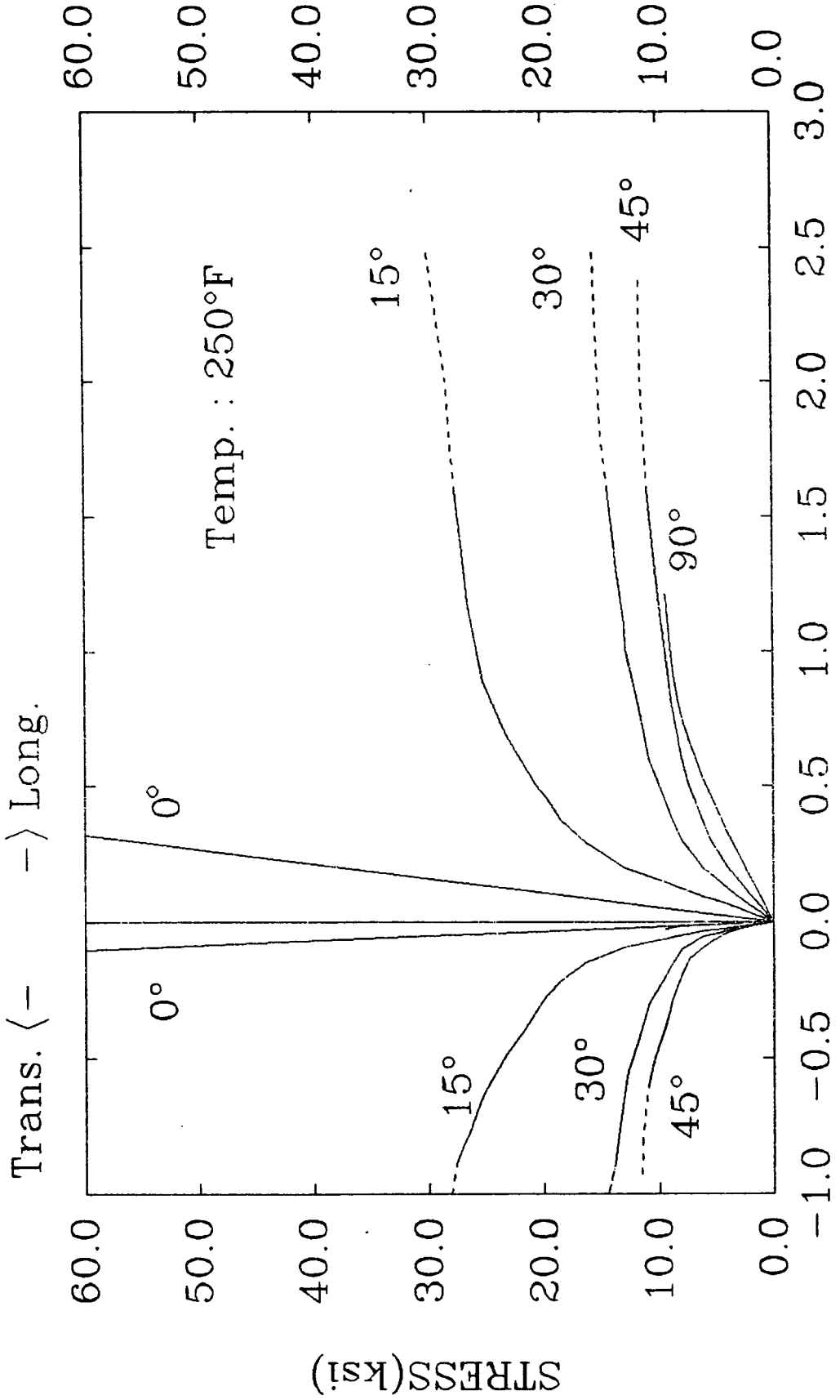

Fig. 3-c. Stress-strain curves for off-axis specimens at 250°F.

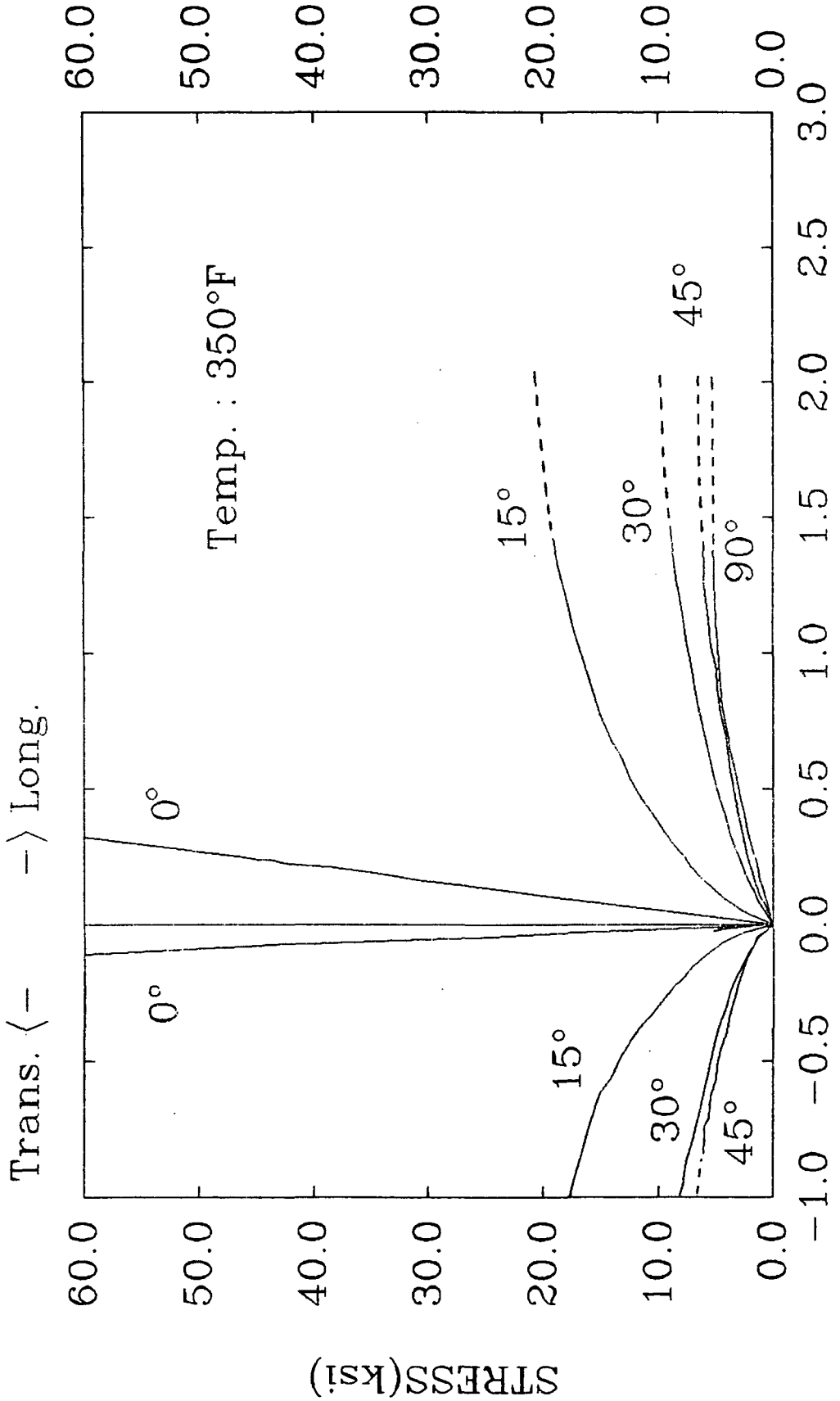

Fig. 3-d. Stress-strain curves for off-axis specimens at 350°F.

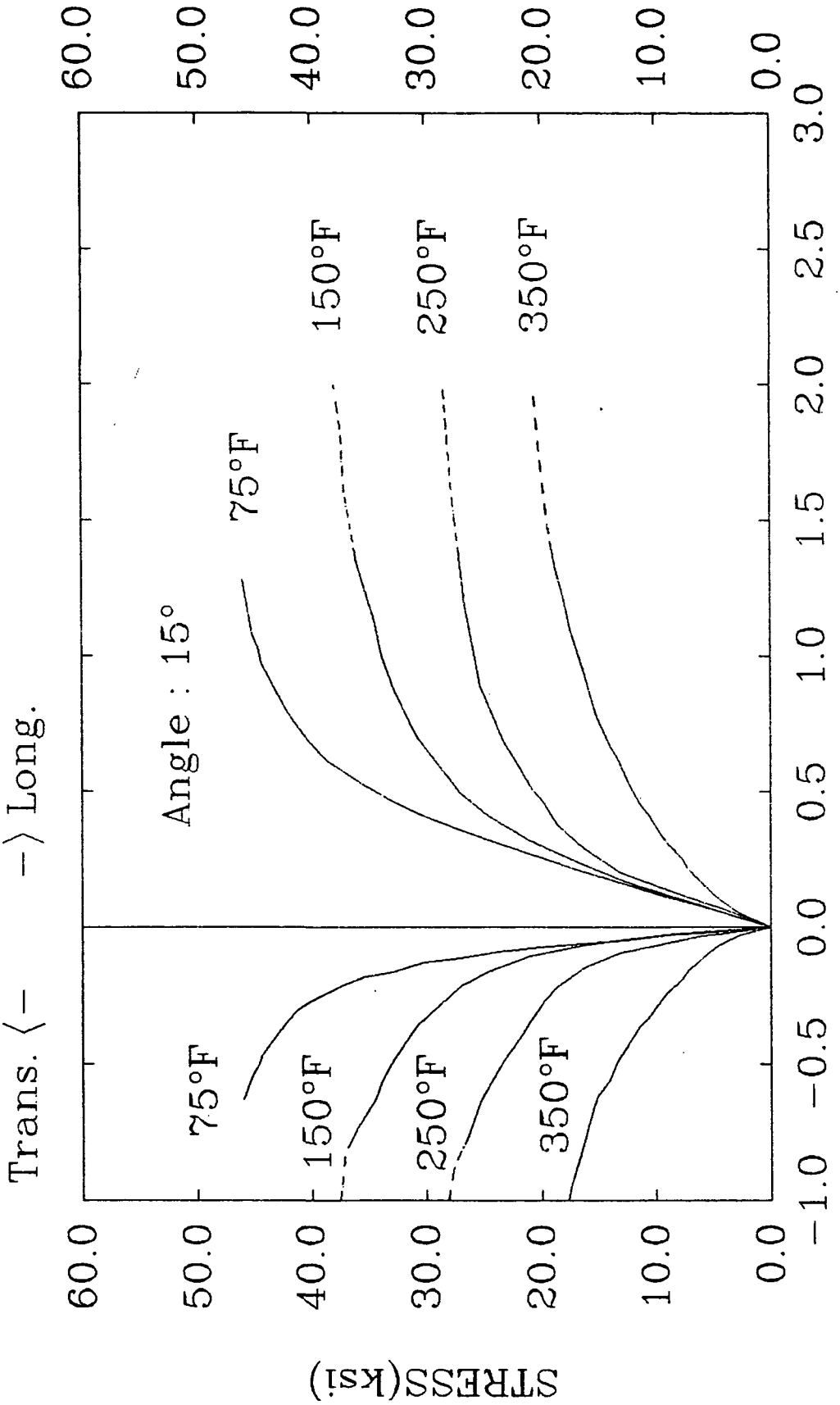

Fig. 4-a. Stress-strain curves for 15° off-axis specimen at various testing temperatures.

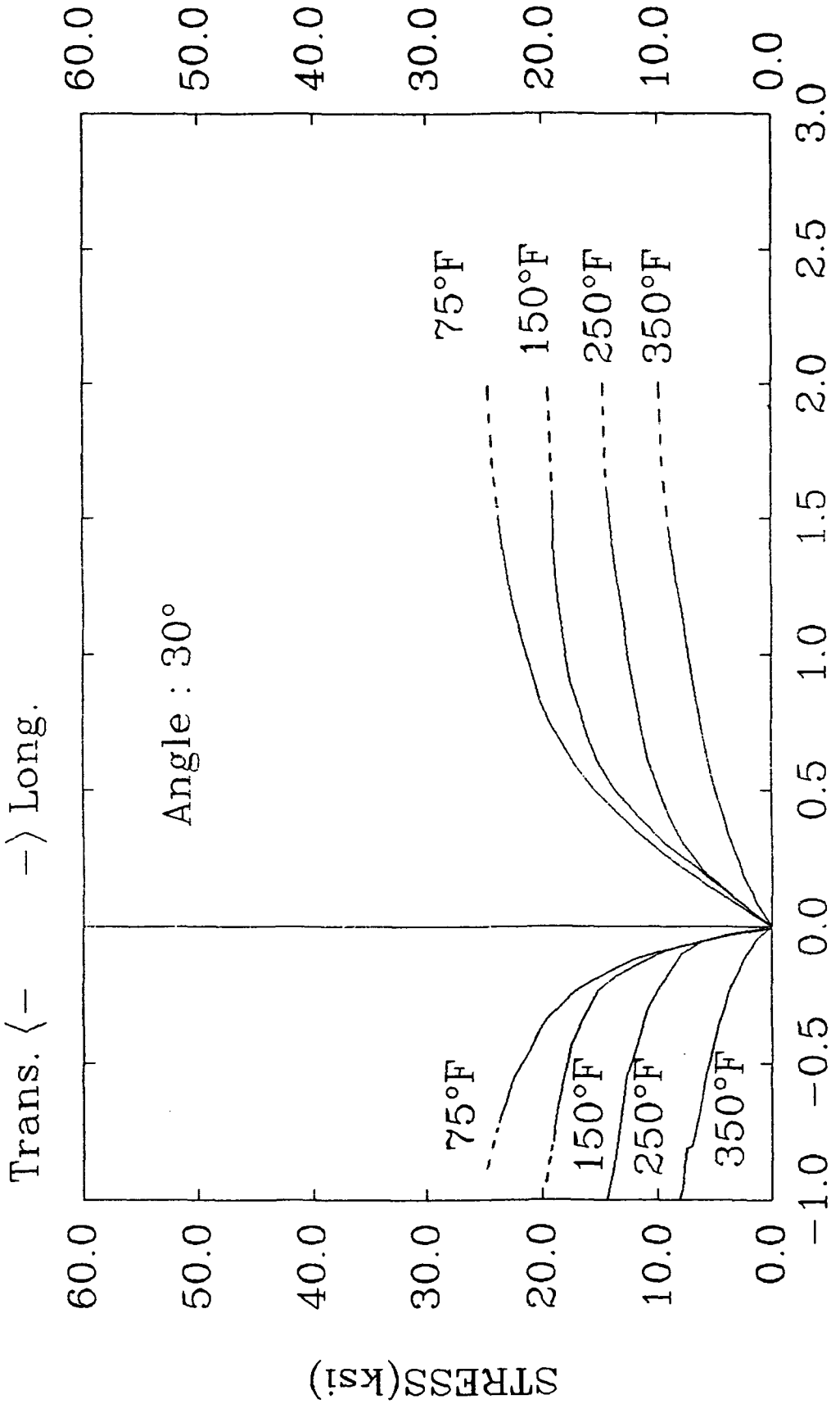

Fig. 4-b. Stress-strain curves for 30° off-axis specimen at various testing temperatures.

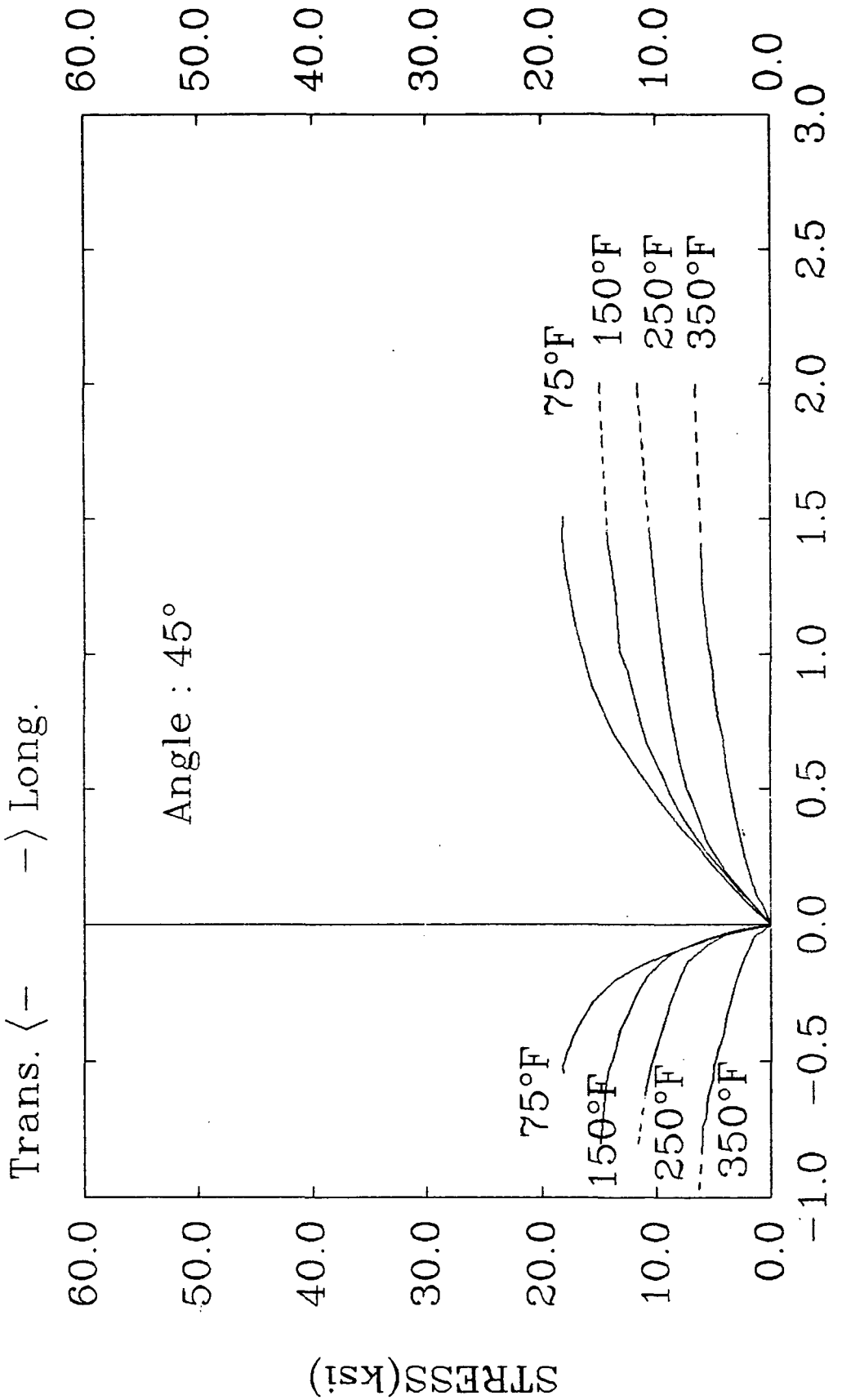

Fig. 4-c. Stress-strain curves for 45° off-axis specimen at various testing temperatures.

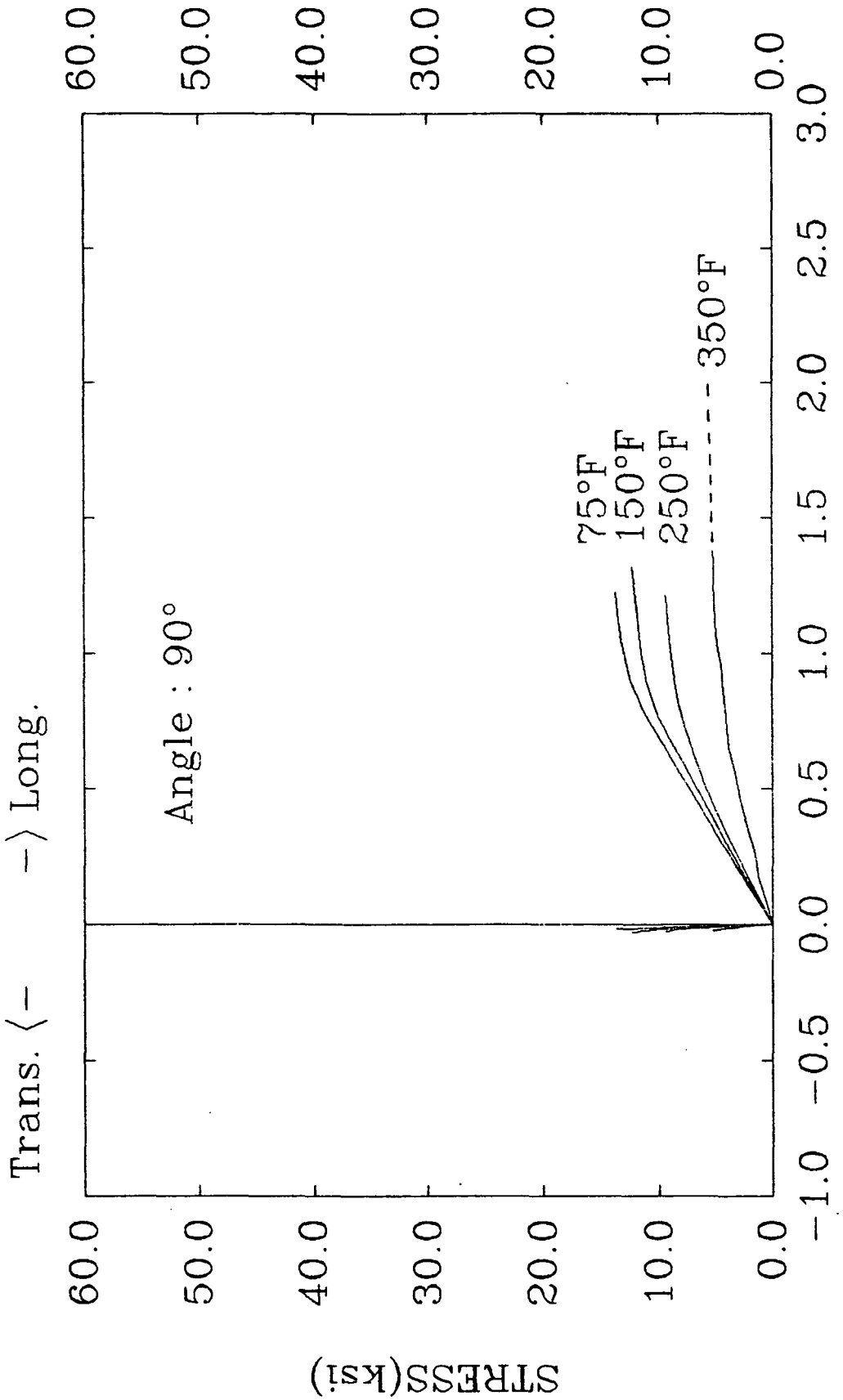

Fig. 4-d. Stress-strain curves for 90° off-axis specimen at various testing temperatures.

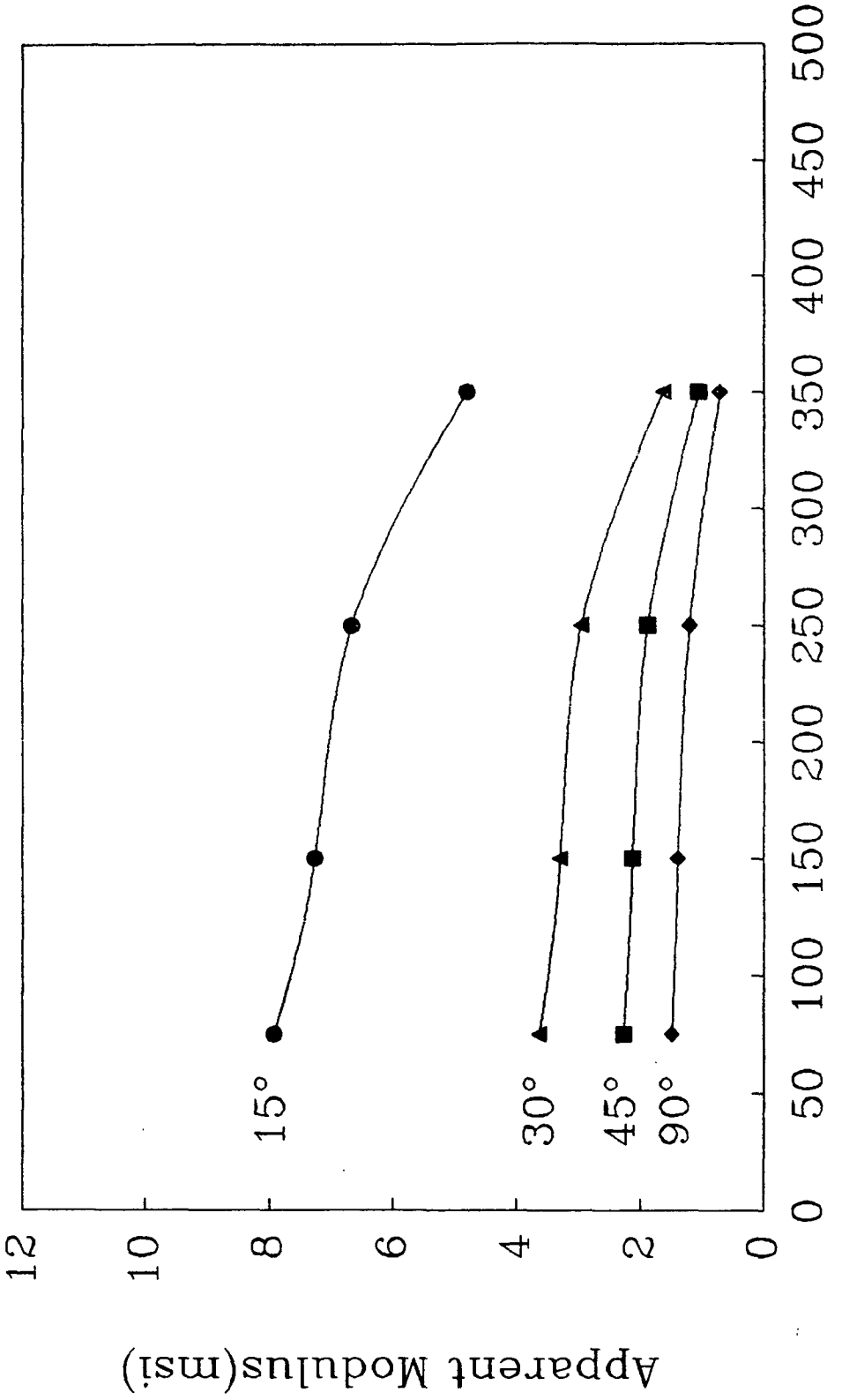

Fig. 5 Variation of apparent elastic moduli with respect to temperature.

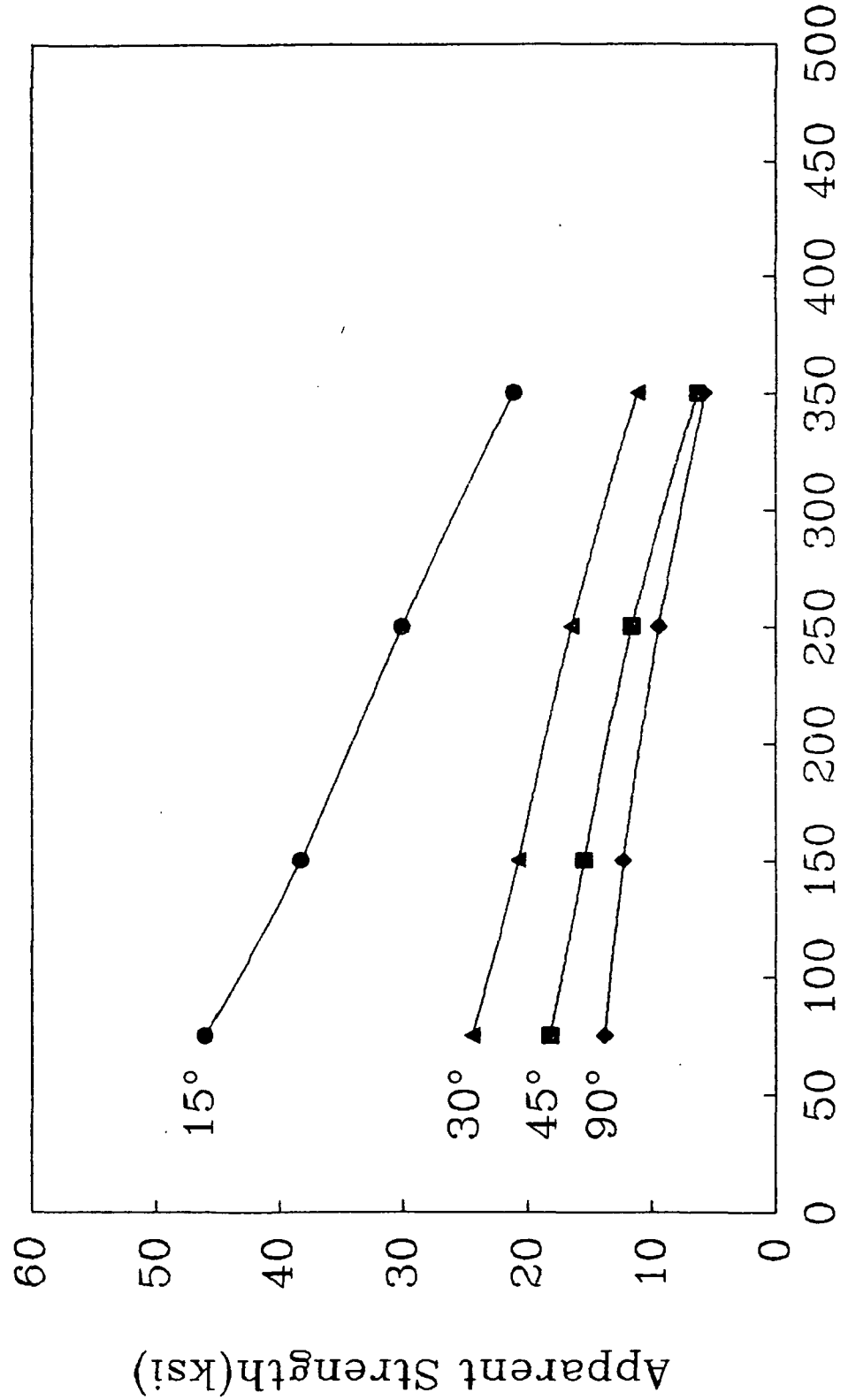

Fig. 6 Variation of apparent strengths with respect to temperature.

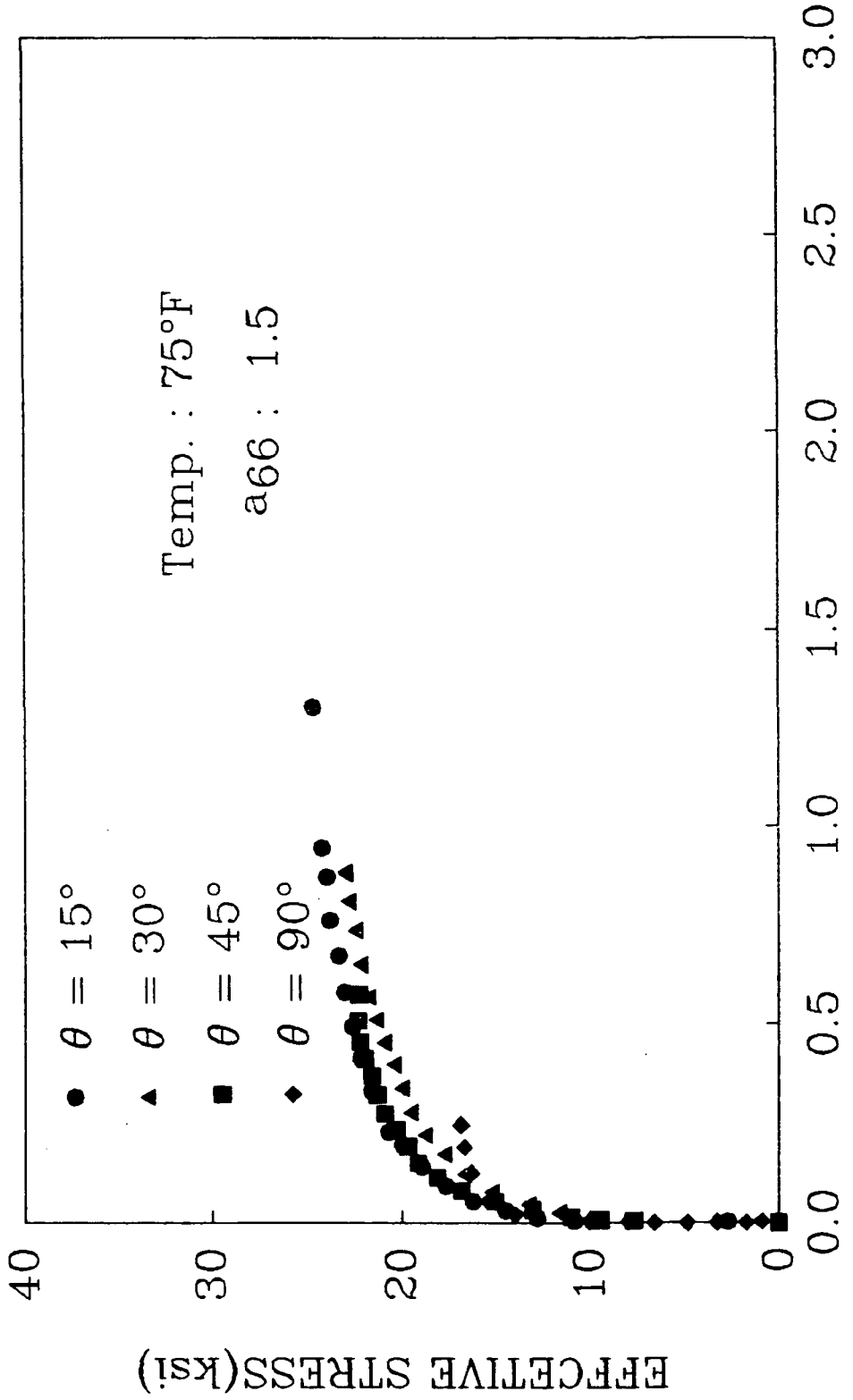

Fig. 7-a. Effective stress and effective plastic strain curves for off-axis specimens with $a_{66} = 1.5$ at 75°F.

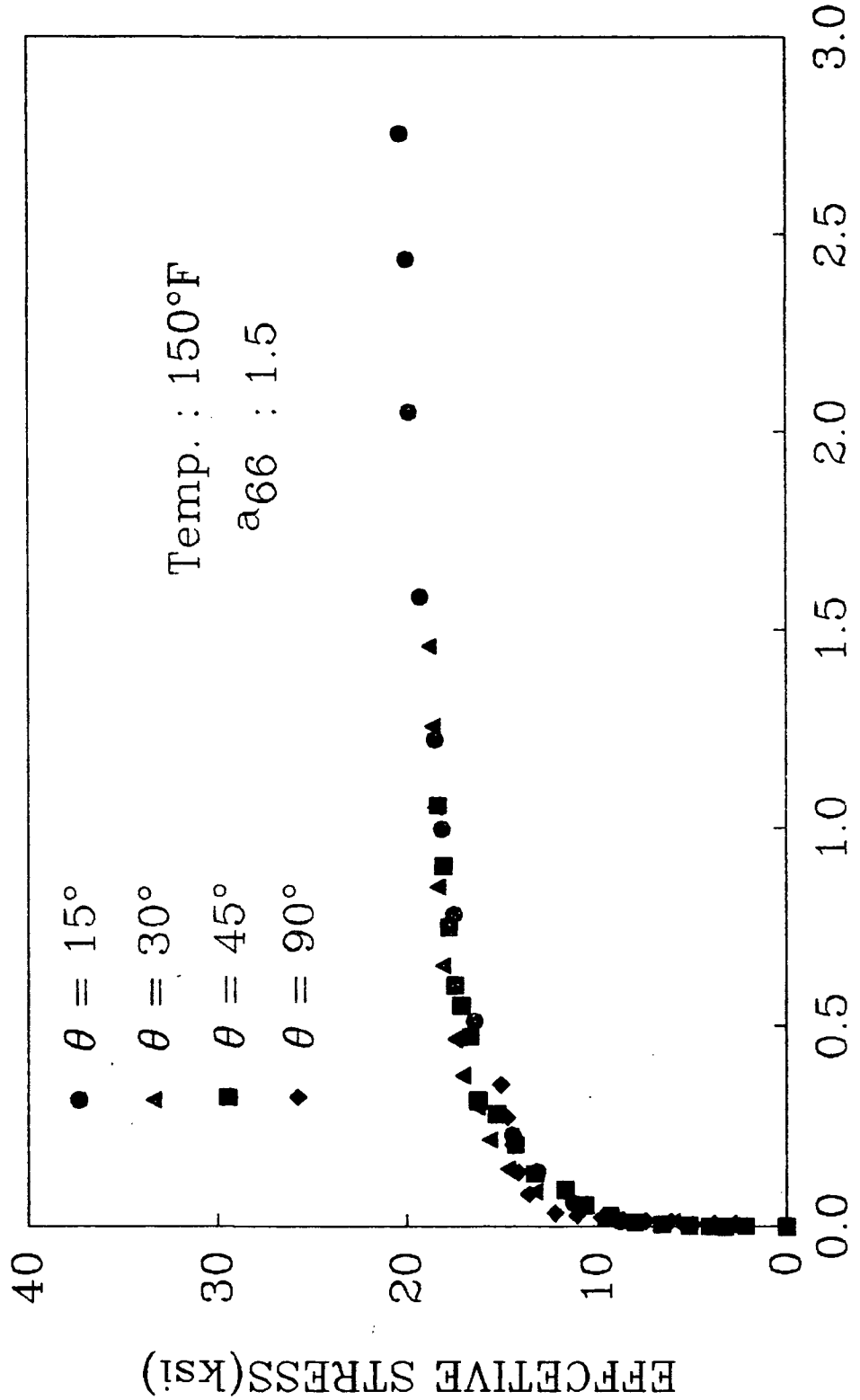

Fig. 7-b. Effective stress-effective plastic strain curves for off-axis specimens with $a_{66} = 1.5$ at 150°F.

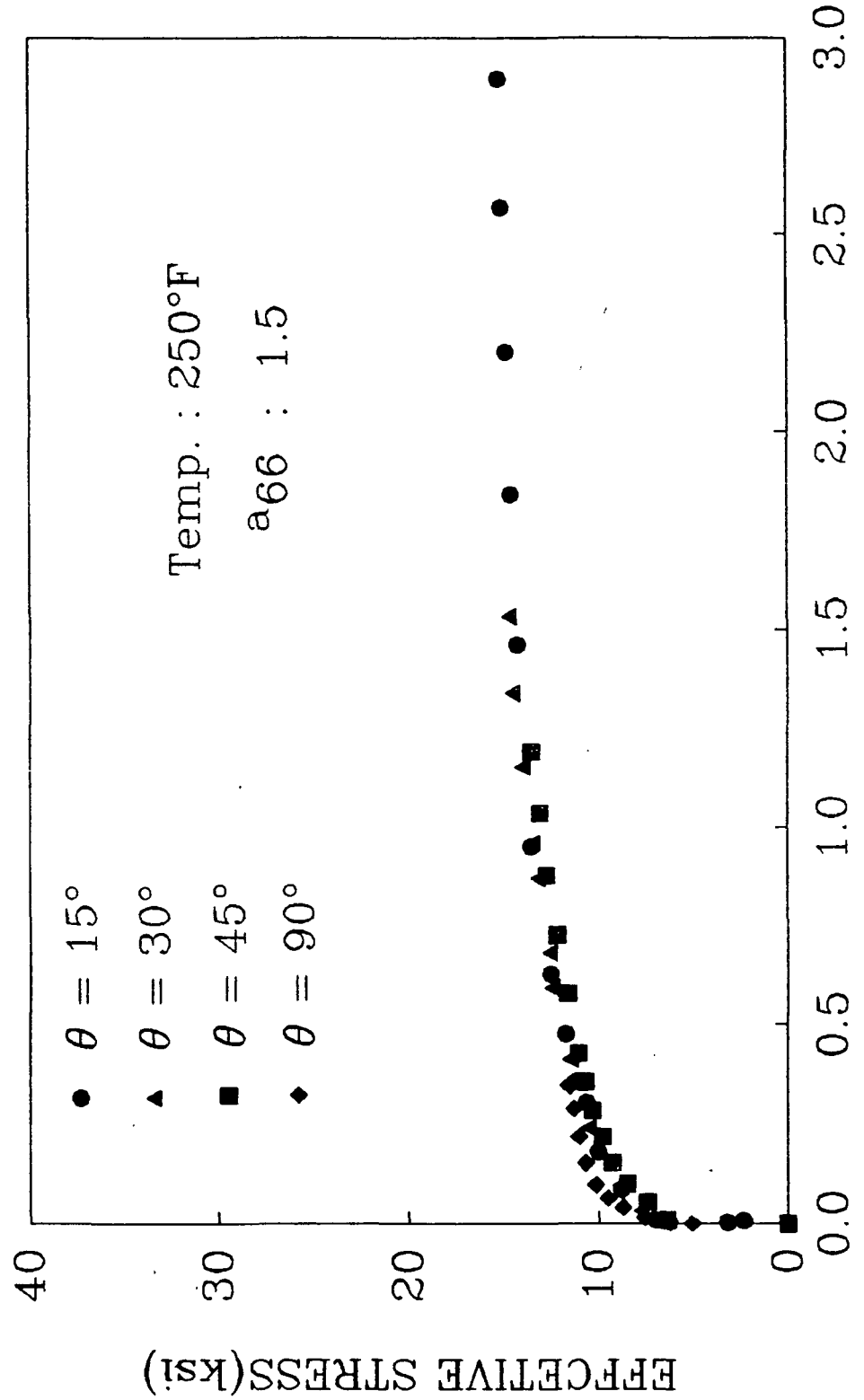

Fig. 7-c. Effective stress-effective plastic strain curves for off-axis specimens with a_{66} = 1.5 at 250°F.

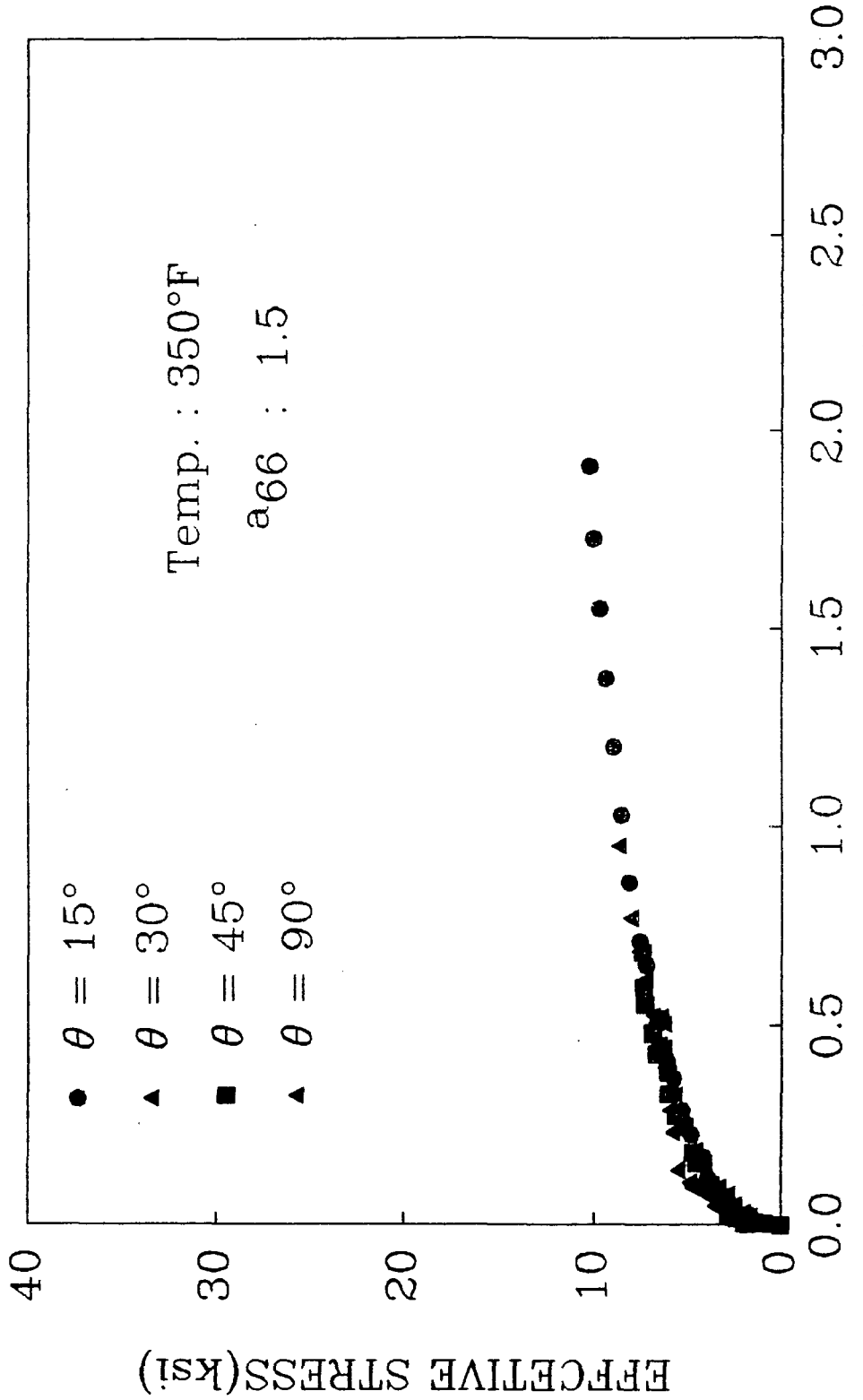

Fig. 7-d. Effective stress-effective plastic strain curves for off-axis specimens with a_{66} = 1.5 at 350°F.

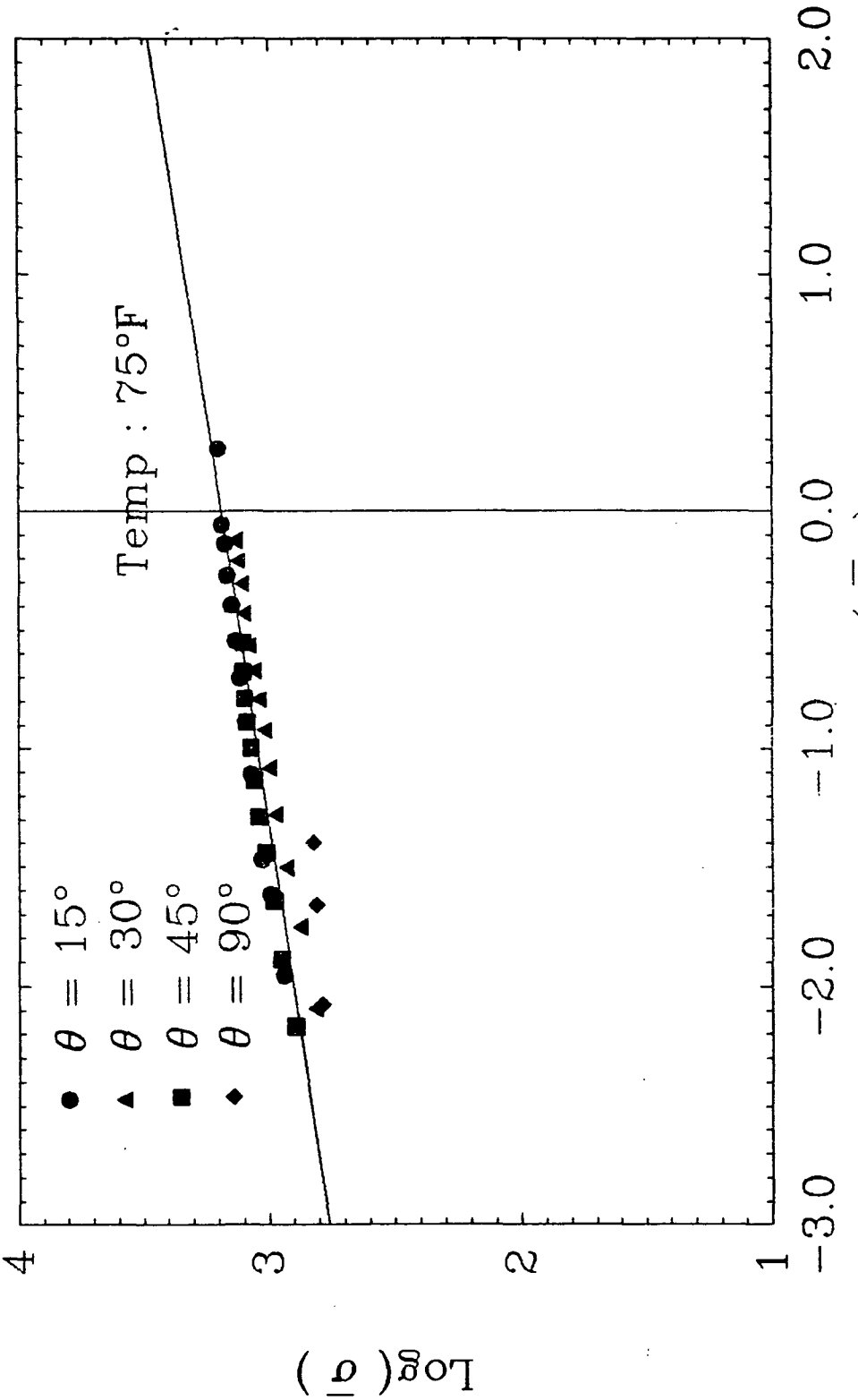

Fig. 8-a. Logarithms of effective stress and effective plastic strain data for off-axis specimens at 75°F.

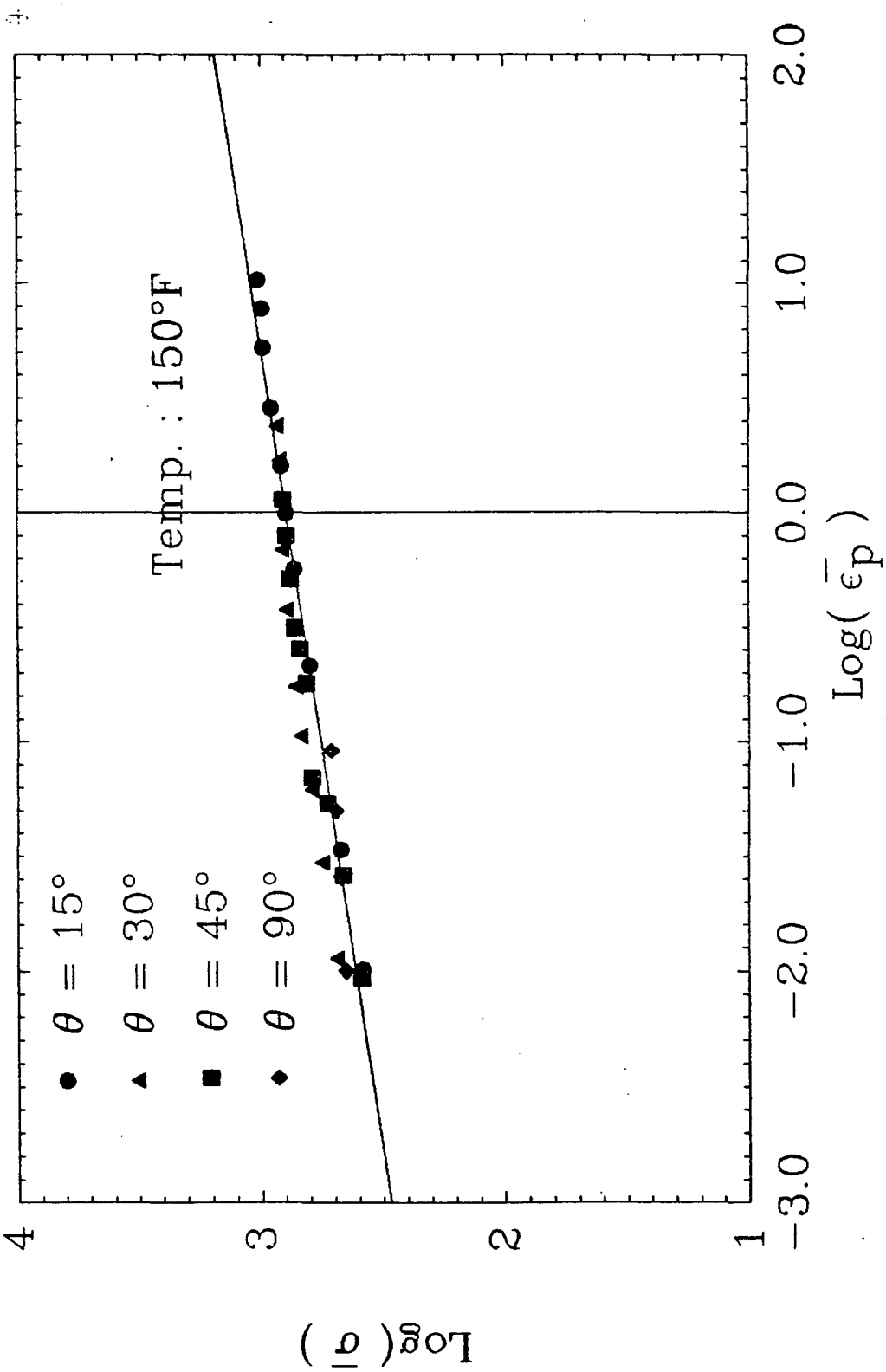

Fig. 8-b. Logarithms of effective stress and effective plastic strain data for off-axis specimens at 150°F.

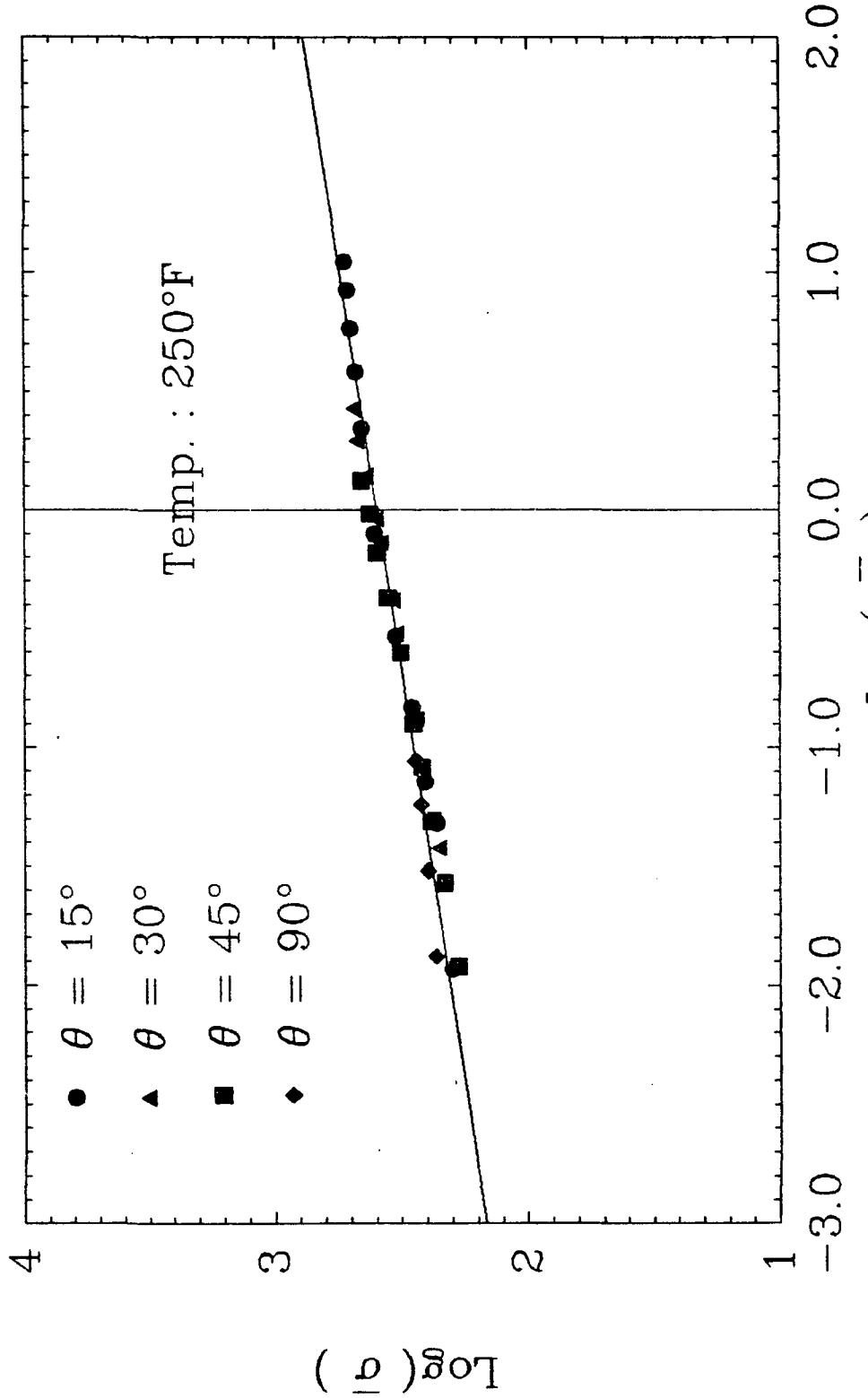

Fig. 8-c. Logarithms of effective stress and effective plastic strain data for off-axis specimens at 250°F.

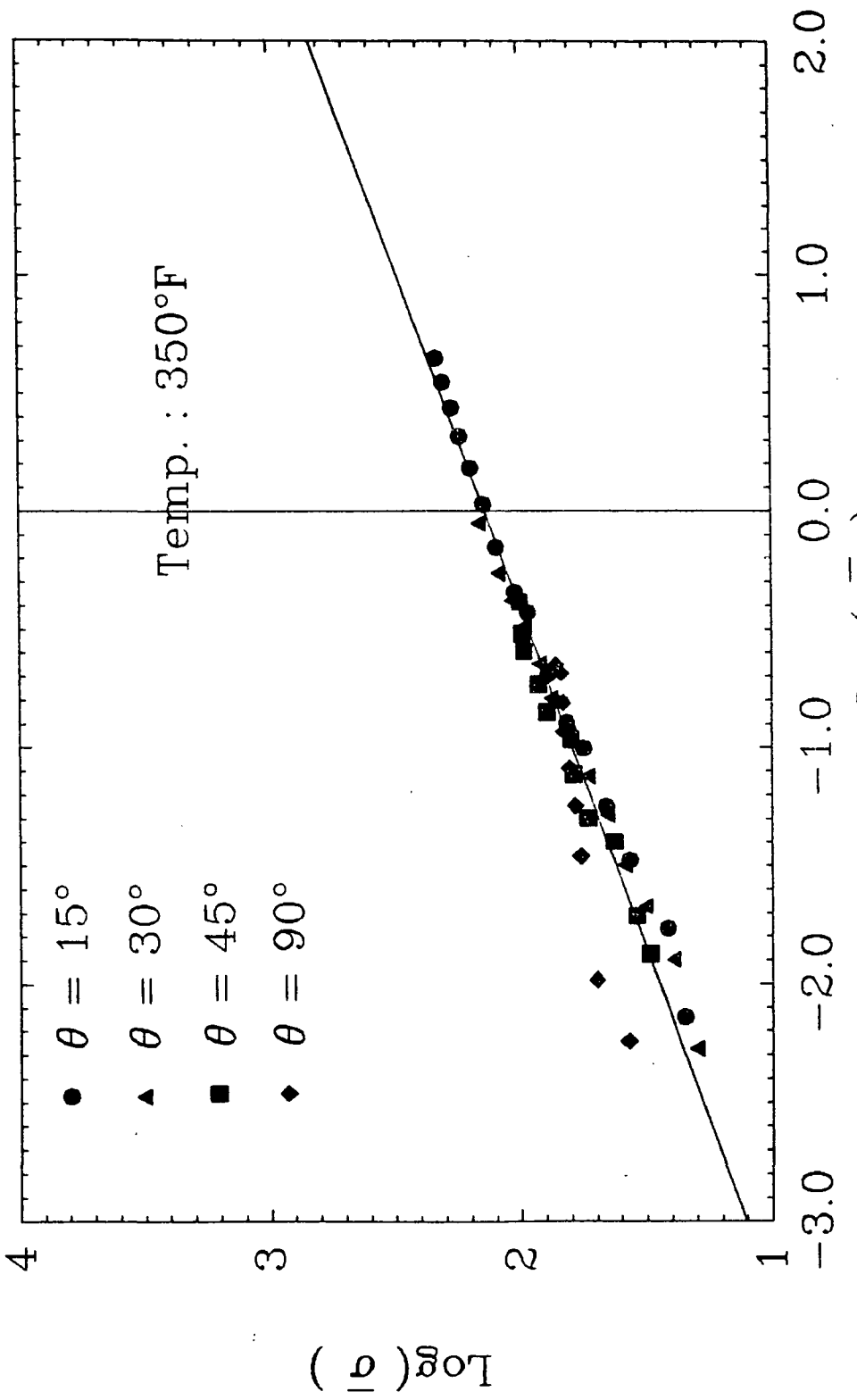

Fig. 8-d. Logarithms of effective stress and effective plastic strain data for off-axis specimen at 350°F.

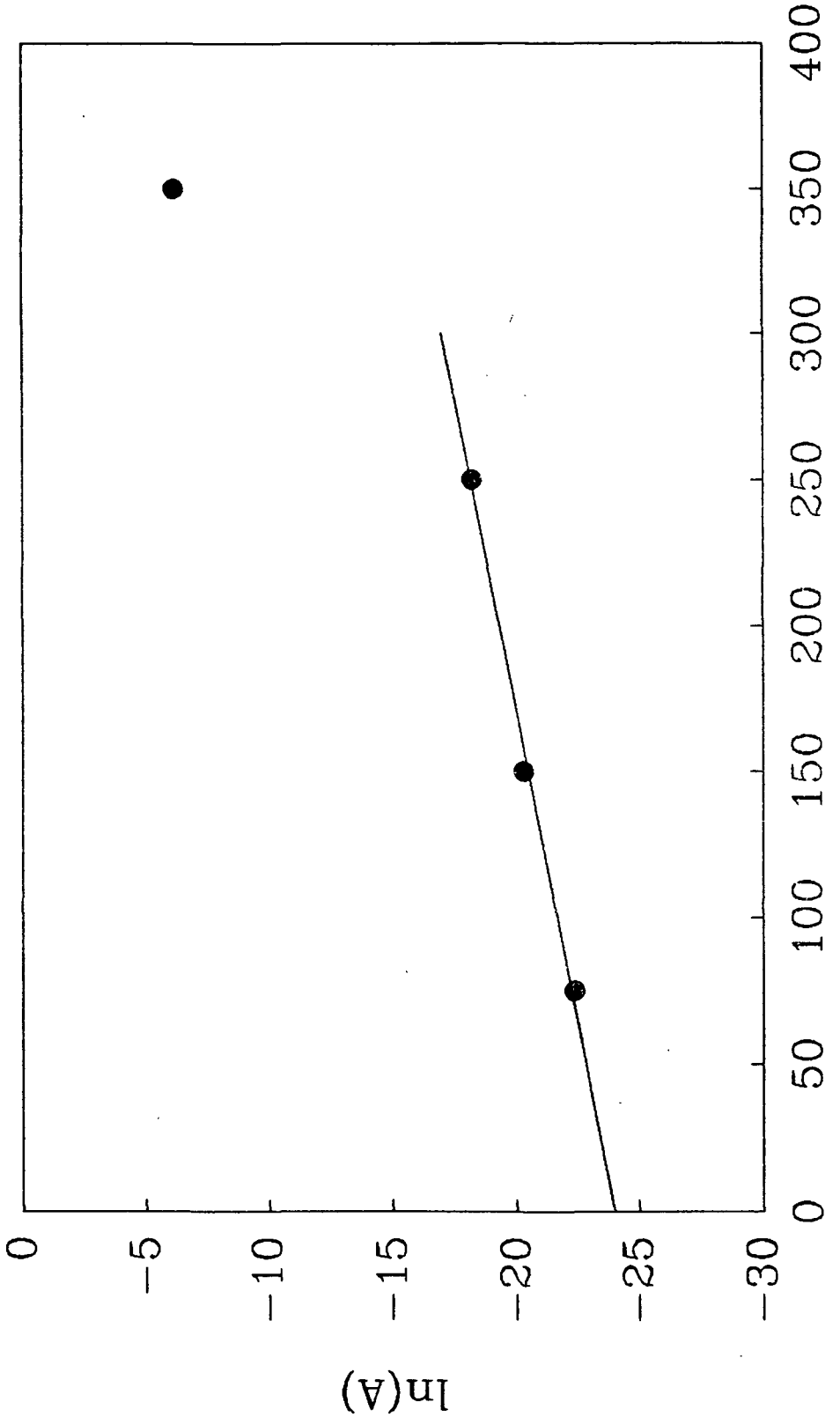

Fig. 9. Logarithms of the coefficient A vs. temperature.

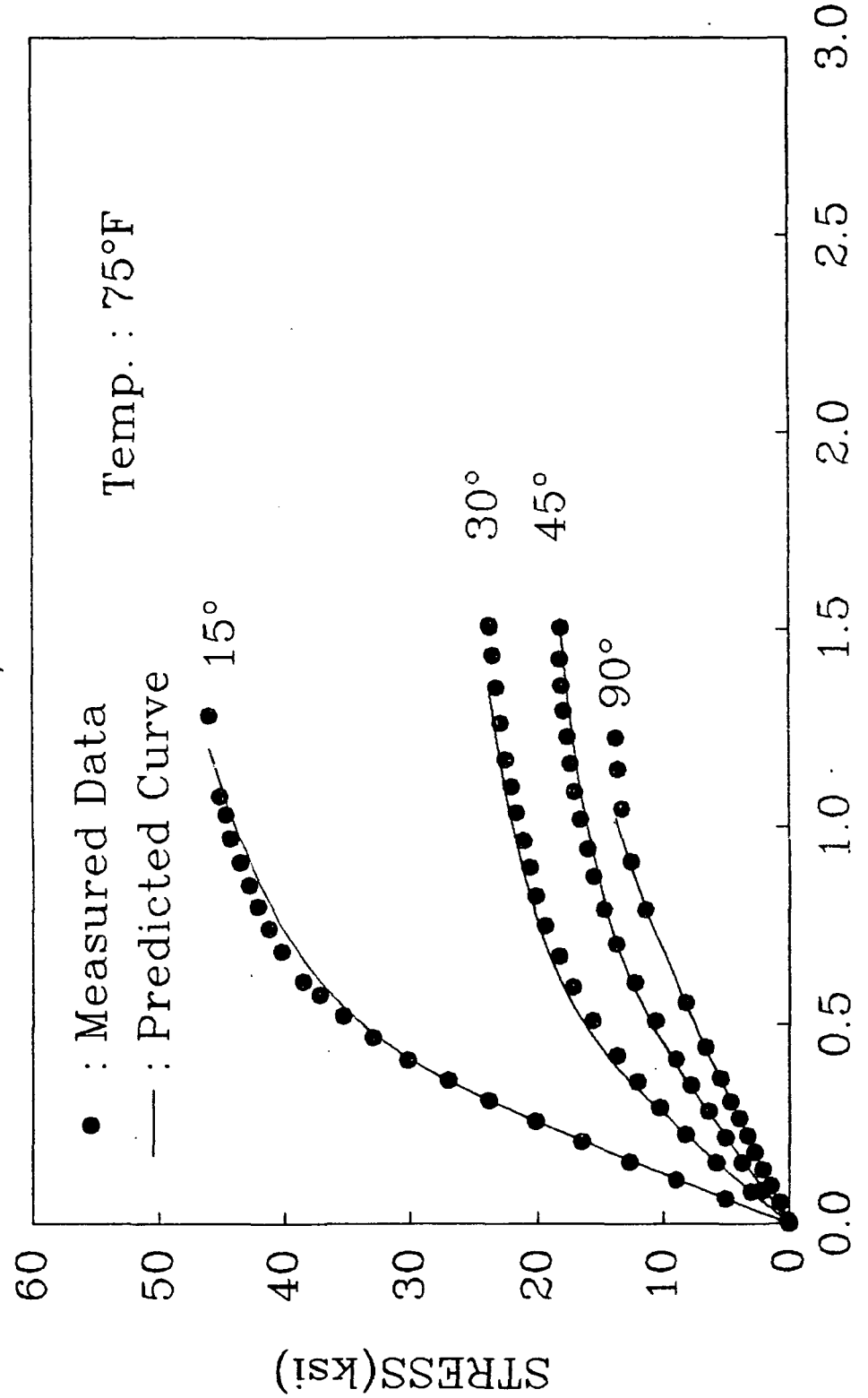

Fig. 10-a. Measured and predicted longitudinal stress-strain curves at 75°F.

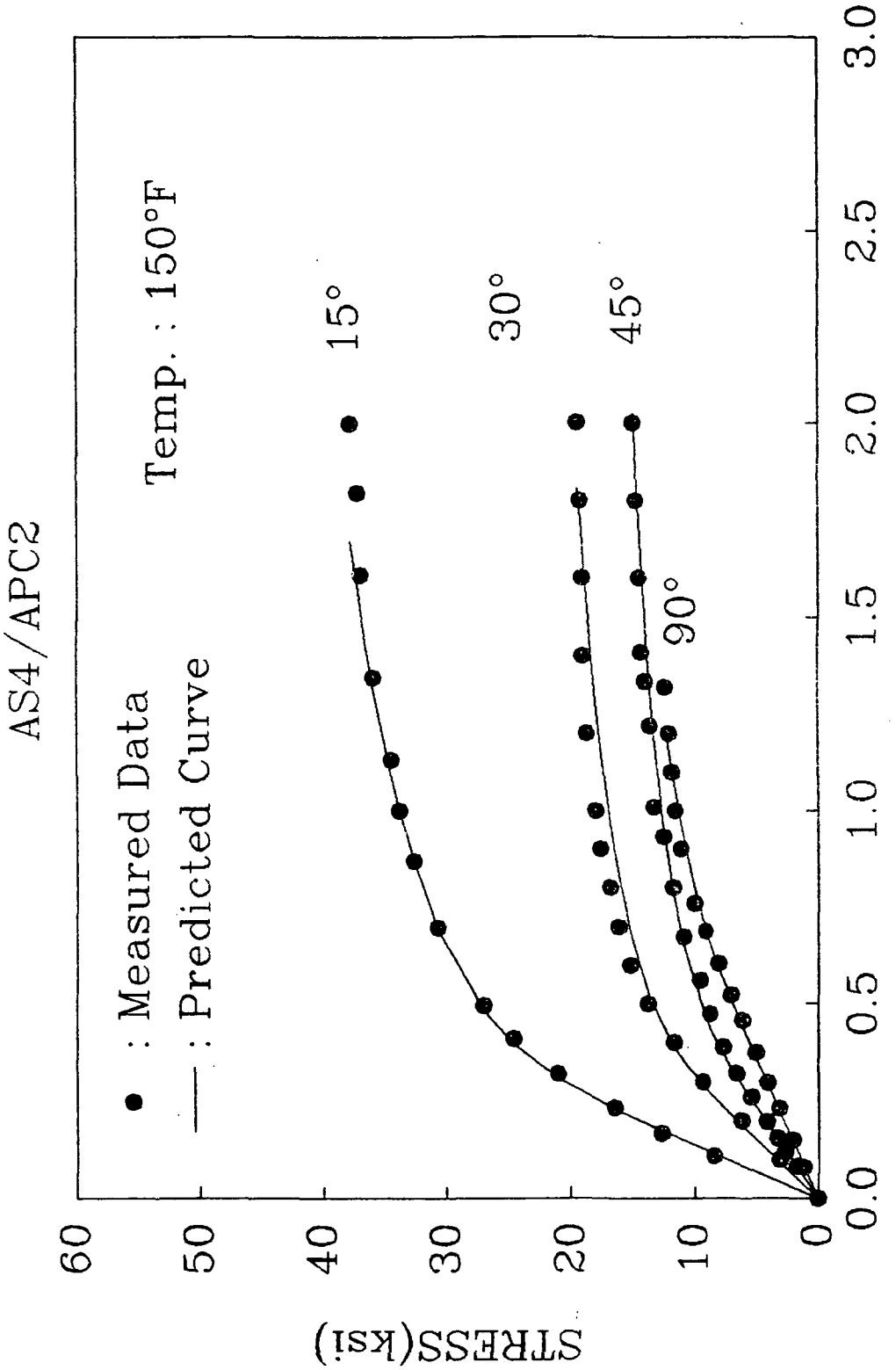

Fig. 10-b. Measured and predicted longitudinal stress-strain curves at 150°F.

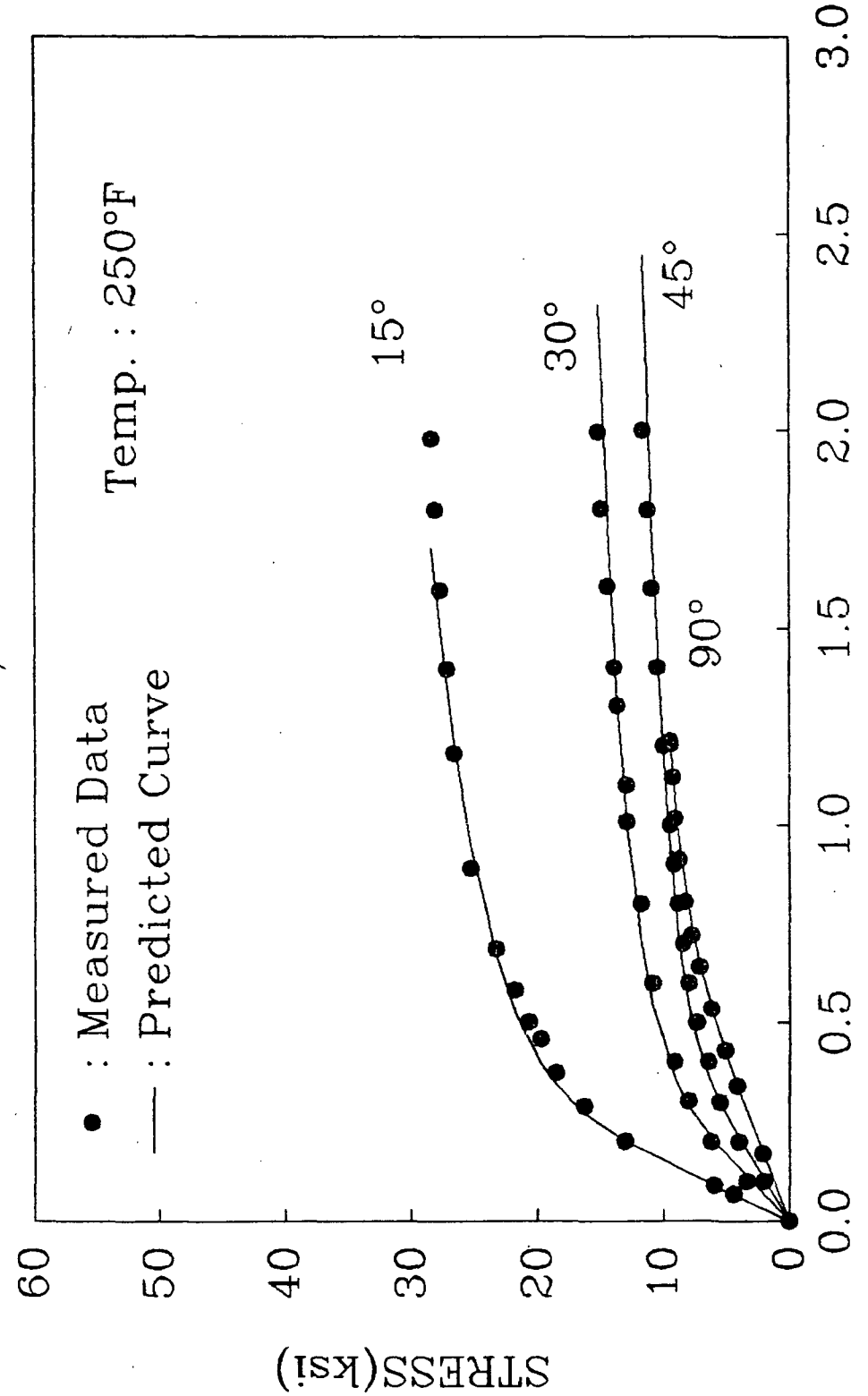

Fig. 10-c. Measured and predicted longitudinal stress-strain curves at 250°F.

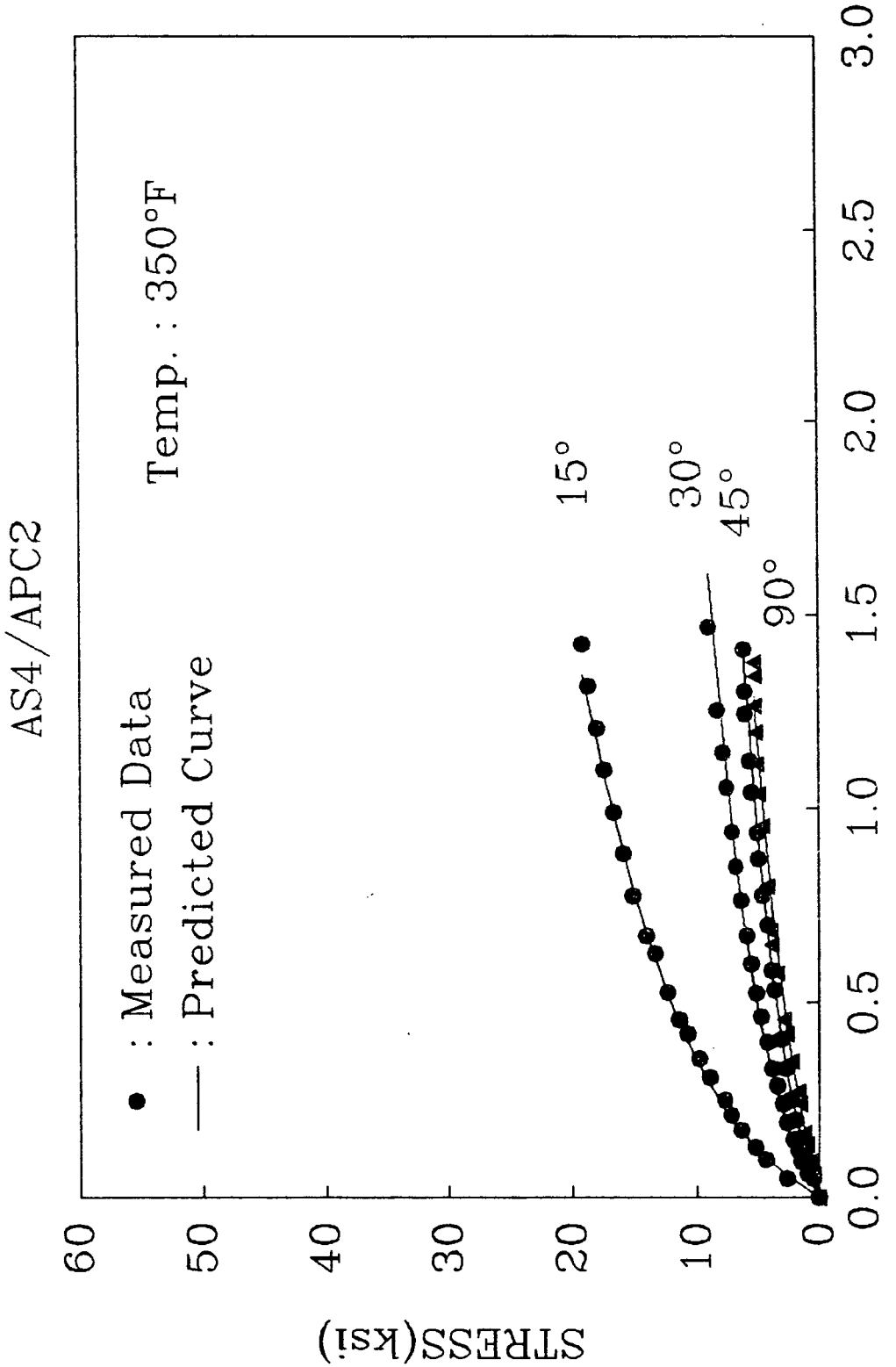

Fig. 10-d. Measured and predicted longitudinal stress-strain curves at 350°F.

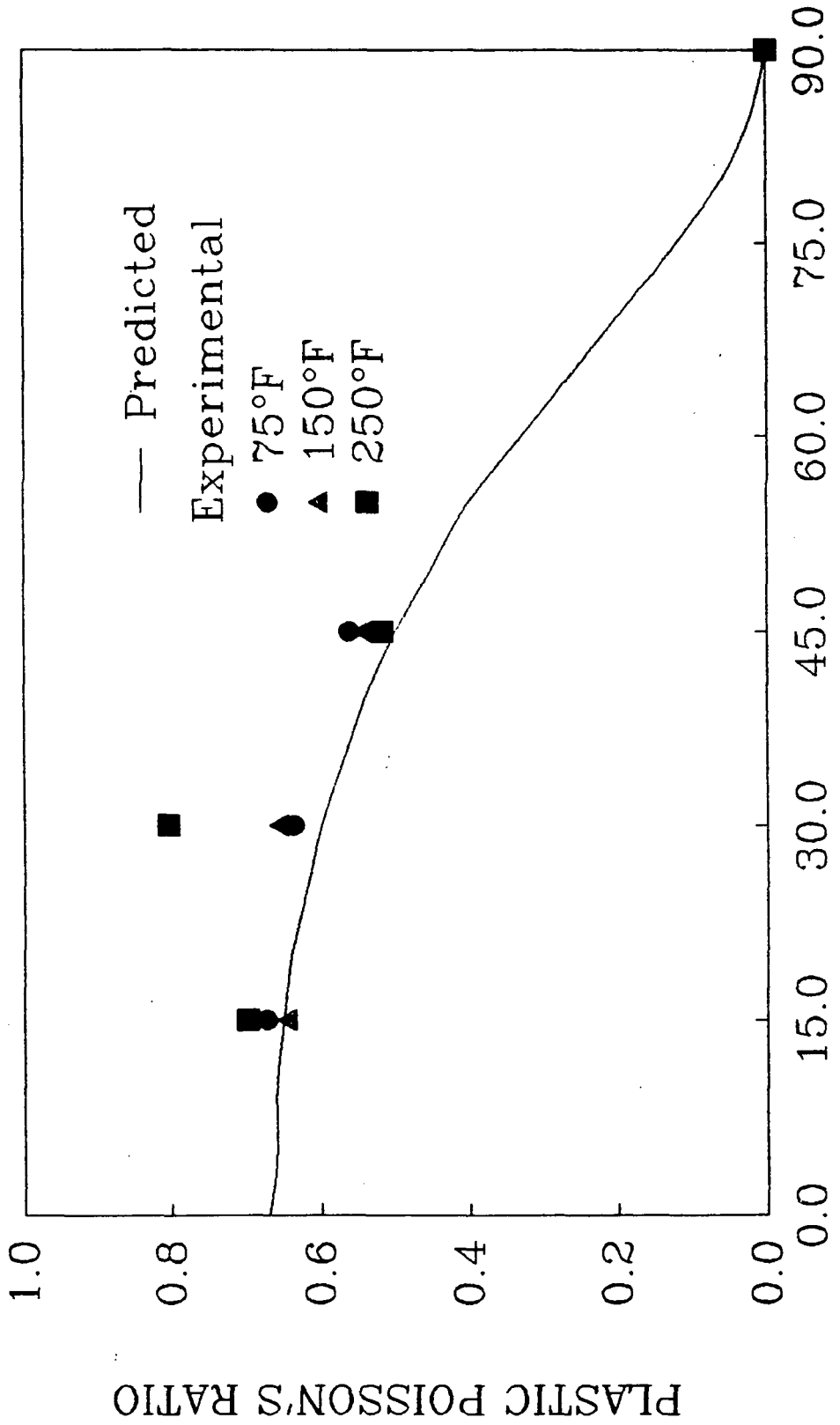

Fig. 11. Measured and predicted plastic Poisson's ratios.

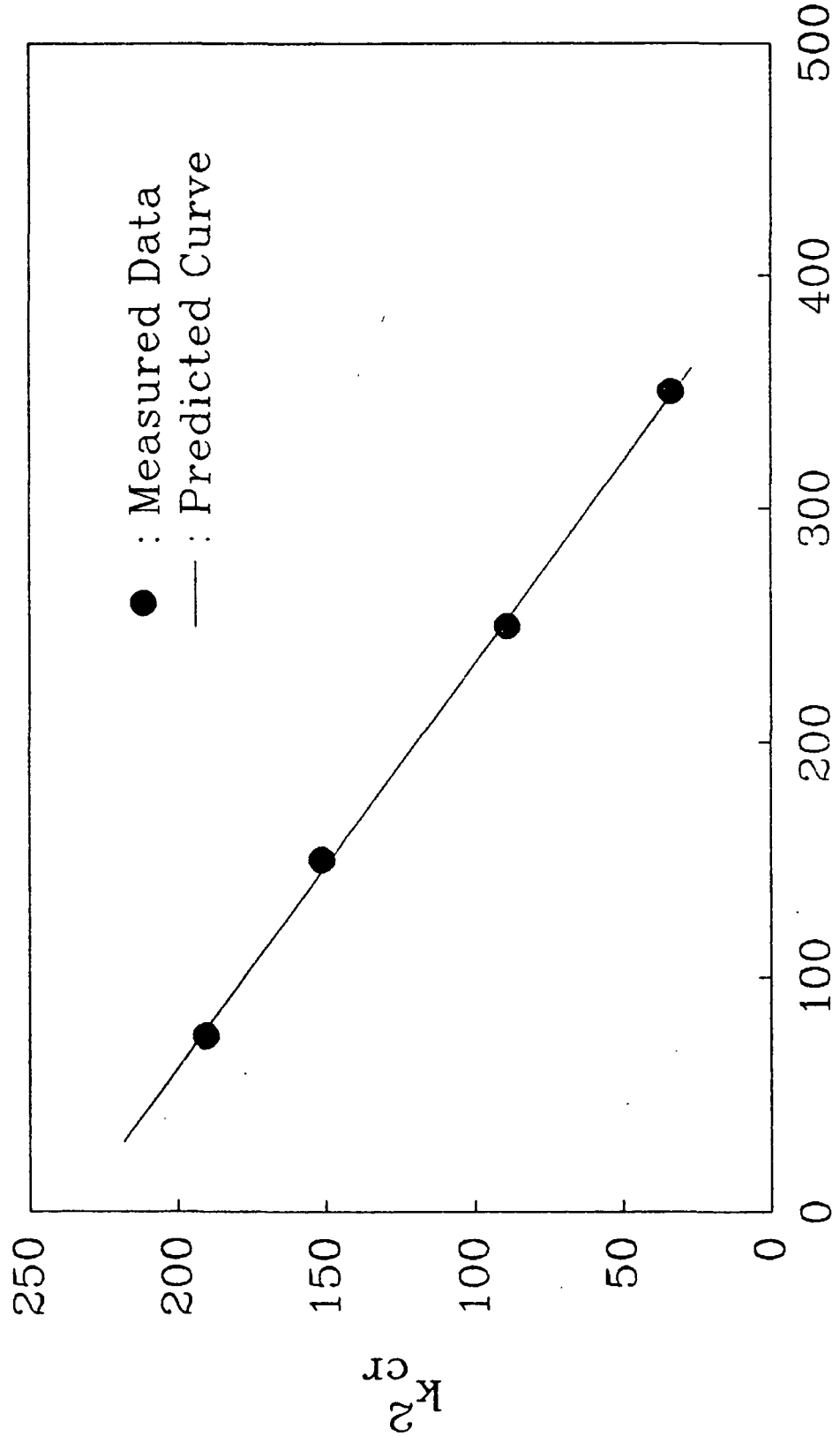

Fig. 12. Variation of k_{cr}^2 vs. temperature.

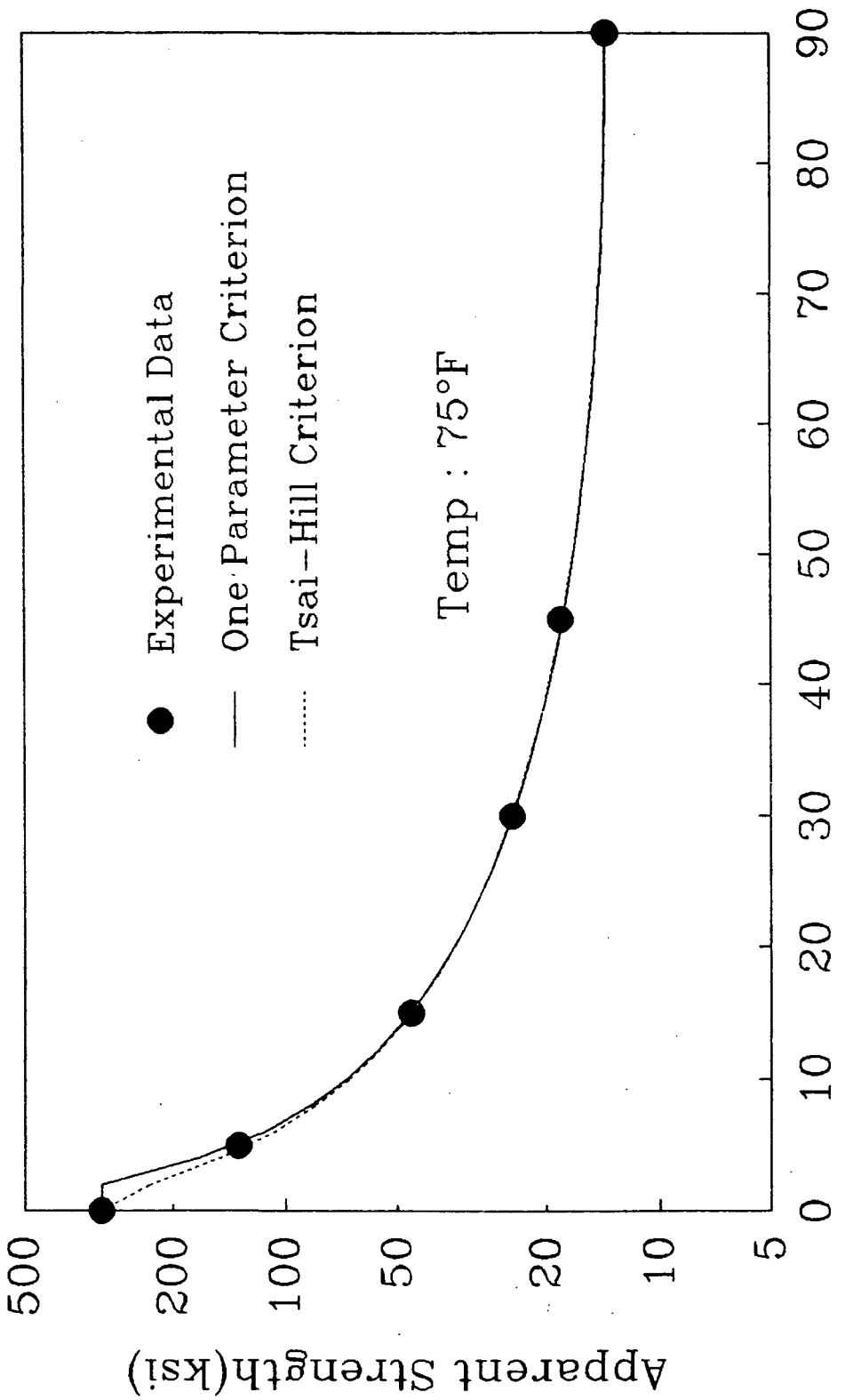

Fig. 13-a. Measured and predicted apparent strengths for off-axis specimens at 75°F.

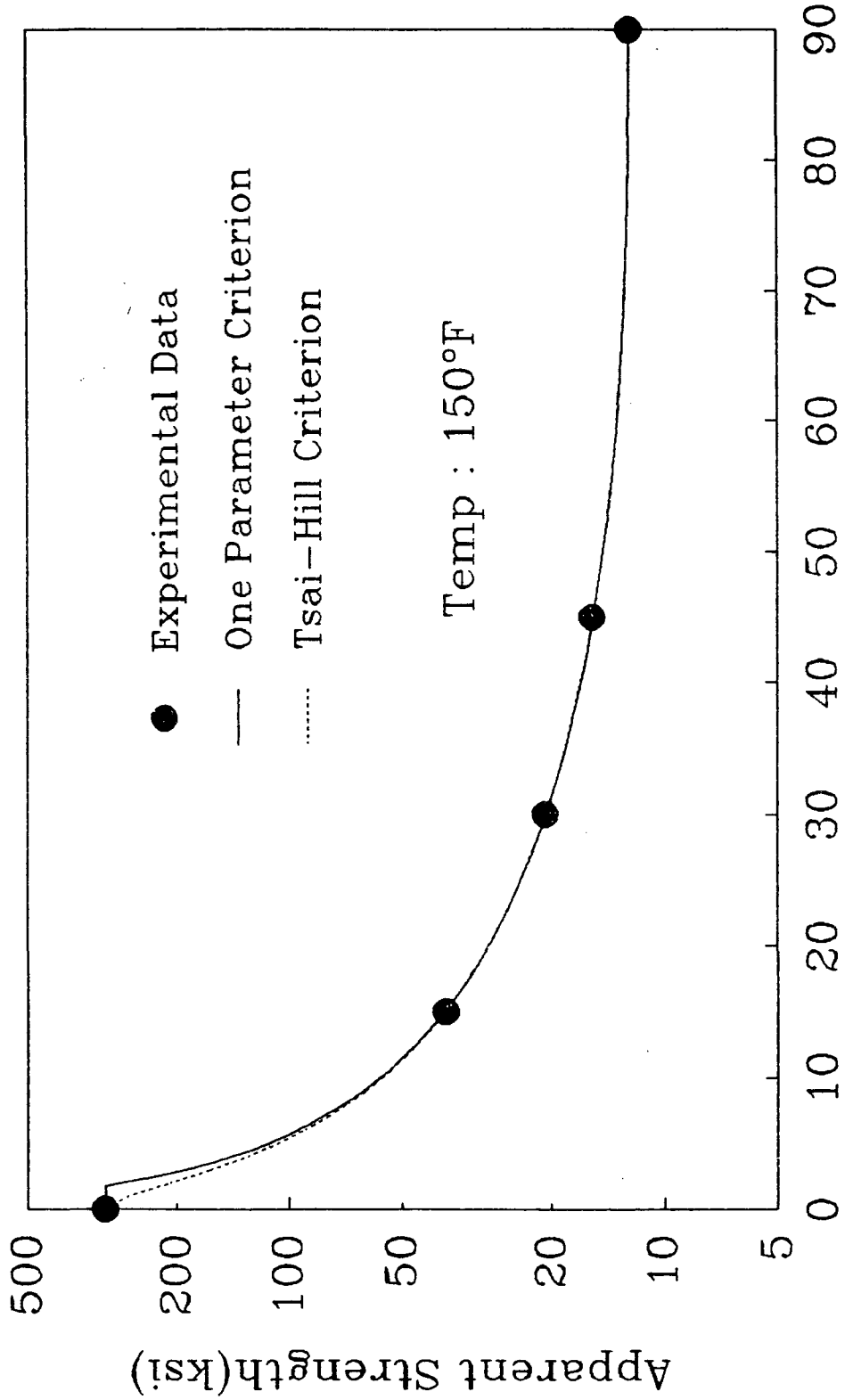

Fig. 13-b. Measured and predicted apparent strengths for off-axis specimens at 150°F.

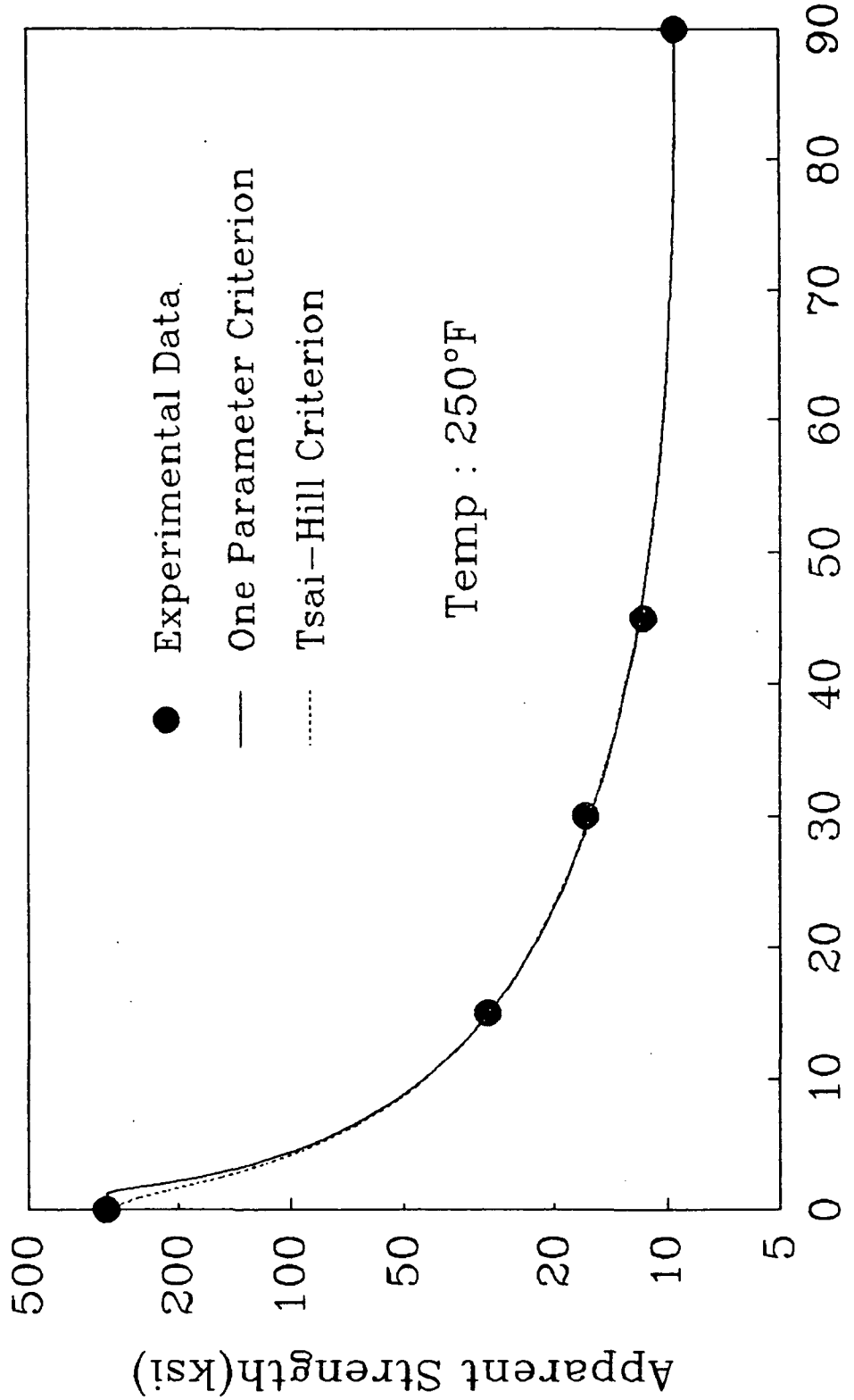

Fig. 13-c. Measured and predicted apparent strengths for off-axis specimens at 250°F.

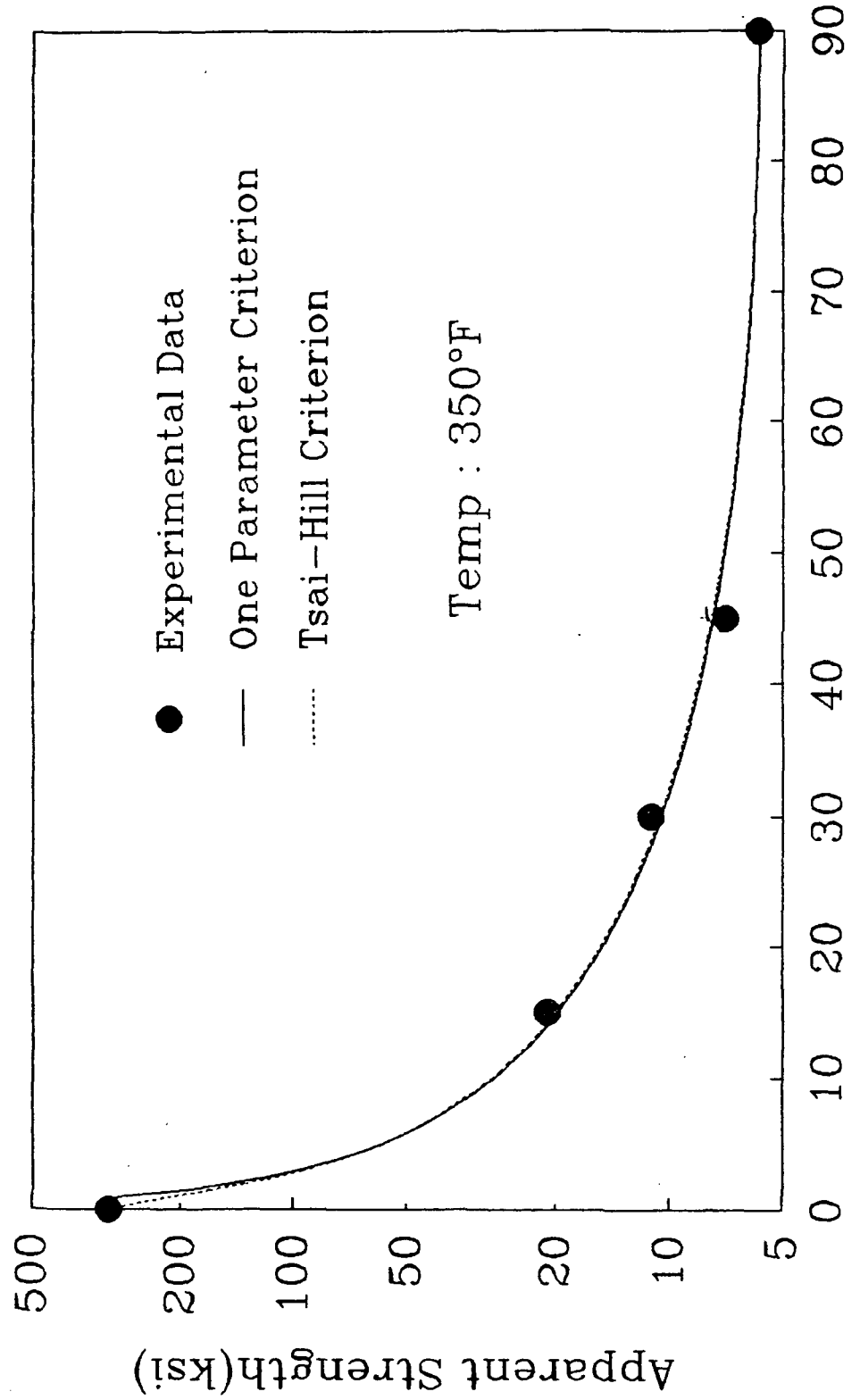

Fig. 13-d. Measured and predicted apparent strengths for off-axis specimens at 350°F.